

AMES  
GRANT  
IN-03-26  
158846  
p. 120

**DESIGN, ANALYSIS, AND CONTROL  
OF LARGE TRANSPORT AIRCRAFT  
UTILIZING ENGINE THRUST AS A BACKUP SYSTEM  
FOR THE PRIMARY FLIGHT CONTROLS**

**SEMI-ANNUAL REPORT IN SUPPORT OF GRANT  
NAG 2-789**

**NATIONAL AERONAUTICS AND SPACE ADMINISTRATION  
DRYDEN FLIGHT RESEARCH FACILITY  
AMES RESEARCH CENTER**

(NASA-CR-192938) DESIGN, ANALYSIS,  
AND CONTROL OF LARGE TRANSPORT  
AIRCRAFT UTILIZING ENGINE THRUST AS  
A BACKUP SYSTEM FOR THE PRIMARY  
FLIGHT CONTROLS (Kansas Univ.)  
120 p

N93-27308

Unclass

G3/08 0158846

**DONNA S. GERREN  
UNIVERSITY OF KANSAS**

**FEBRUARY 1993**

## TABLE OF CONTENTS

<u>Subject</u>	<u>Page</u>
LIST OF SYMBOLS.....	iv
LIST OF TABLES.....	ix
LIST OF FIGURES.....	xii
1. CHAPTER 1 - INTRODUCTION.....	1
1.1. DOUGLAS DC-10 UNITED AIRLINES ACCIDENT.....	1
1.2. NATIONAL TRANSPORTATION SAFETY BOARD RECOMMENDATIONS.....	5
1.3. STUDIES REGARDING USE OF THROTTLES FOR EMERGENCY FLIGHT CONTROL.....	6
1.4. PURPOSE AND OBJECTIVES.....	7
2. CHAPTER 2 - BACKGROUND INFORMATION.....	13
2.1. INTRODUCTION.....	13
2.2. AIRCRAFT INCIDENTS WITH SIGNIFICANT FLIGHT CONTROL FAILURES.....	14
2.2.1. DOUGLAS DC-10 AMERICAN AIRLINES INCIDENT.....	15
2.2.2. DOUGLAS DC-10 TURKISH AIRLINES ACCIDENT.....	16
2.2.3. LOCKHEED C-5A USAF ACCIDENT.....	16
2.2.4. LOCKHEED L-1011 DELTA AIRLINES INCIDENT.....	17
2.2.5. BOEING 747 JAPAN AIRLINES ACCIDENT.....	19
2.3. PRINCIPLES OF ENGINES-ONLY CONTROL.....	20
2.3.1. YAW-ROLL CONTROL.....	20
2.3.2. PITCH CONTROL.....	21
2.3.2.1. PHUGOID OSCILLATIONS.....	21

## TABLE OF CONTENTS (CON'T)

<u>Subject</u>	<u>Page</u>
2.3.2.2. FLIGHT PATH ANGLE CHANGE RESULTING FROM SPEED STABILITY.....	23
2.3.2.3. PITCHING MOMENT RESULTING FROM THRUST LINE OFFSET.....	24
2.3.2.4. FLIGHT PATH ANGLE CHANGE RESULTING FROM THE VERTICAL COMPONENT OF THRUST.....	24
2.3.3. SPEED CONTROL.....	24
2.3.4. THRUST RESPONSE.....	25
2.3.5. EFFECTS OF THRUST ON PROPULSIVE CONTROL POWER.....	25
2.4. HISTORICAL REVIEW.....	26
2.4.1. FLIGHT RESEARCH STUDIES.....	27
2.4.1.1. F-15 AIR SUPERIORITY FIGHTER.....	27
2.4.1.2. LEAR 24 EXECUTIVE JET TRANSPORT.....	28
2.4.1.3. PA-30 PISTON-POWERED LIGHT TWIN- ENGINE PLANE.....	29
2.4.2. SIMULATOR STUDIES.....	30
2.4.2.1. B-720 COMMERCIAL JET TRANSPORT.....	30
2.4.2.2. B-727 COMMERCIAL JET TRANSPORT.....	31
2.4.2.3. F-15 AIR SUPERIORITY FIGHTER.....	32
2.4.2.4. MD-11 COMMERCIAL JET TRANSPORT.....	33
2.4.3. OVERALL FLYING QUALITIES.....	33

## TABLE OF CONTENTS (CON'T)

<u>Subject</u>	<u>Page</u>
2.4.3.1. AUGMENTED CONTROL SYSTEM.....	34
2.5. CURRENT RESEARCH.....	37
3. CHAPTER 3 - OUTLINE OF PROPOSED WORK.....	49
3.1. INTRODUCTION.....	49
3.2. FAMILIARIZATION WITH PREVIOUS NASA WORK AND APPLICABLE NASA RESEARCH TOOLS.....	51
3.3. BASELINE DESIGN OF A MEGA-TRANSPORT.....	54
3.3.1. MISSION SPECIFICATIONS.....	54
3.3.2. MISSION PROFILE.....	55
3.3.3. SUMMARY OF THE MEGA-TRANSPORT DATA.....	57
3.4. DEVELOP A SIMULATION OF THE MEGA-TRANSPORT.....	57
3.5. MEGA-TRANSPORT SIMULATION FLYING QUALITIES EVALUATION.....	58
3.6. MEGA-TRANSPORT SIMULATION FLYING QUALITIES ANALYSIS.....	59
3.7. DETERMINATION OF BENEFITS ASSOCIATED WITH AUGMENTED THROTTLES-ONLY CONTROL SYSTEM.....	64
4. CHAPTER 4 - REFERENCES.....	97

## LIST OF SYMBOLS

<u>Symbol</u>	<u>Definition</u>	<u>Dimension</u>
$\alpha$	Angle of attack	deg or rad
AR	Aspect ratio	-----
b	Span	ft
c.g.	Center of gravity	-----
C	Chord	ft
$C_D$	Drag coefficient	-----
$C_{D_u}$	Drag due to speed	-----
$C_{D_\alpha}$	Drag due to angle of attack	rad <sup>-1</sup>
$C_{D_{\delta_e}}$	Drag due to elevator	rad <sup>-1</sup>
$C_{l_p}$	Rolling moment due to roll rate	rad <sup>-1</sup>
$C_{l_r}$	Rolling moment due to yaw rate	rad <sup>-1</sup>
$C_{l_\beta}$	Rolling moment due to sideslip	rad <sup>-1</sup>
$C_{l_{\delta_a}}$	Rolling moment due to aileron	rad <sup>-1</sup>
$C_{l_{\delta_r}}$	Rolling moment due to rudder	rad <sup>-1</sup>
$C_L$	Lift coefficient	-----
$C_{L_q}$	Lift due to pitch rate	rad <sup>-1</sup>
$C_{L_u}$	Lift due to speed	-----
$C_{L_\alpha}$	Lift due to angle of attack	rad <sup>-1</sup>
$C_{L_{\alpha \dot{\alpha}}}$	Lift due to rate of angle of attack	rad <sup>-1</sup>
$C_{L_{\delta_e}}$	Lift due to elevator	rad <sup>-1</sup>
$C_m$	Pitching moment coefficient	-----
$C_{m_q}$	Pitching moment due to pitch rate	rad <sup>-1</sup>
$C_{m_T}$	Thrust pitching moment coefficient	-----
$C_{m_{T_u}}$	Thrust pitching moment due to speed	-----
$C_{m_{T_\alpha}}$	Thrust pitching moment due to angle of attack	-----

## LIST OF SYMBOLS (CON'T)

<u>Symbol (con't)</u>	<u>Definition</u>	<u>Dimension</u>
$C_{m_u}$	Pitching moment due to speed	-----
$C_{m_\alpha}$	Pitching moment due to angle of attack	rad <sup>-1</sup>
$C_{m_{\dot{\alpha}}}$	Pitching moment due to rate of angle of attack	rad <sup>-1</sup>
$C_{m_{\delta_e}}$	Pitching moment due to elevator	rad <sup>-1</sup>
$C_{n_p}$	Yawing moment due to roll rate	rad <sup>-1</sup>
$C_{n_r}$	Yawing moment due to yaw rate	rad <sup>-1</sup>
$C_{n_\beta}$	Yawing moment due to sideslip	rad <sup>-1</sup>
$C_{n_{\delta_a}}$	Yawing moment due to aileron	rad <sup>-1</sup>
$C_{n_{\delta_r}}$	Yawing moment due to rudder	rad <sup>-1</sup>
$C_{T_X}$	Thrust force coefficient	-----
$C_{T_{X_u}}$	Thrust due to speed	-----
$C_{y_p}$	Side force due to roll rate	rad <sup>-1</sup>
$C_{y_r}$	Side force due to yaw rate	rad <sup>-1</sup>
$C_{y_\beta}$	Side force due to sideslip	rad <sup>-1</sup>
$C_{y_{\delta_a}}$	Side force due to aileron	rad <sup>-1</sup>
$C_{y_{\delta_r}}$	Side force due to rudder	rad <sup>-1</sup>
$D$	Diameter	ft
$H_N$	Frequency response of neuro- muscular dynamics	-----
$H_p$	Human pilot transfer function	-----
$I_{xxB}$	Moment of inertia about X- body axis	slug-ft <sup>2</sup>
$I_{xzB}$	Product of inertia	slug-ft <sup>2</sup>
$I_{yyB}$	Moment of inertia about Y- body axis	slug-ft <sup>2</sup>

## LIST OF SYMBOLS (CON'T)

<u>Symbol (con't)</u>	<u>Definition</u>	<u>Dimension</u>
I <sub>zzB</sub>	Moment of inertia about Z-body axis	slug-ft <sup>2</sup>
j	Square root of -1	-----
K	Gain constant	-----
L	Length	ft
M	Mach number	-----
n	Load factor or Laplace variable	-----
n m	Nautical miles	n m
p	Perturbed roll rate	rad/sec
q	Perturbed pitch rate	rad/sec
r	Perturbed yaw rate	rad/sec
s	Laplace variable	sec <sup>-1</sup>
S	Area	ft <sup>2</sup>
T	Thrust	lb
T <sub>eng</sub>	Time constant of engine	sec
u	Perturbed forward velocity	ft/sec
v	Perturbed side velocity	ft/sec
V	True airspeed	mph, fps, or kts
VC	Calibrated airspeed	kts
V <sub>p</sub>	Velocity of the c.g.	ft/sec
w	Perturbed downward velocity	ft/sec
W	Weight	lb
x	Distance along X	ft

## LIST OF SYMBOLS (CON'T)

<u>Greek Symbol</u>	<u>Definition</u>	<u>Dimension</u>
$\alpha$	Angle of attack	rad or deg
$\beta$	Sideslip angle	rad or deg
$\gamma$	Flight path angle	rad or deg
$\delta, \Delta$	Incremental value	-----
$\zeta$	Damping ratio	
$\theta$	Pitch attitude angle	rad or deg
$\lambda$	Taper ratio	
$\Lambda$	Sweep angle	deg
$\tau$	Time constant	sec
$\tau_L$	Lead time constant of the pilot	sec
$\phi$	Bank (roll) angle	rad or deg
$\omega$	Frequency	rad/sec or deg/sec
$\omega_n, \omega_o$	Undamped natural frequency	rad/sec or deg/sec

<u>Subscripts</u>	<u>Definition</u>
cl	Climb
clean	Clean
cr	Cruise
crew	Crew
den	Denominator
D	Dutch roll
e	Equivalent
E	Empty
fus	Fuselage
F	Fuel
h	Horizontal tail
L	Landing
max	Maximum
num	Numerator



## LIST OF SYMBOLS (CON'T)

### Subscripts (con't)

### Definition

p	Pilot
P	Phugoid
PL	Payload
r	Root
reqd	Required
R	Roll
S	Spiral
SP	Short-period
t	Tip
tfo	Trapped fuel and oil
TO	Takeoff
v	Vertical tail
w	Wing
1	Steady state

### Acronyms

### Definition

AAA	Advanced Aircraft Analysis
AIAA	American Institute of Aeronautics and Astronautics
CAS	Control Augmentation System
DAC	Douglas Aircraft Company
FAA	Federal Aviation Administration
FAR	Federal Aviation Regulations
LDP	Landing Difficulty Parameter
NASA	National Aeronautics and Space Administration
NTSB	National Transportation Safety Board
PCA	Propulsion Controlled Aircraft
PIO	Pilot Induced Oscillation
PLA	Power Lever Angle
PLF	Power for Level Flight
USAF	United States Air Force

## LIST OF TABLES

<u>Table</u>	<u>Title</u>	<u>Page</u>
2.1	Physical Characteristics of the Airplanes	39
3.1	Classification of Airplanes	66
3.2	Flight Phase Categories	67
3.3	Levels of Flying Qualities	69
3.4	Allowable Probability of Certain System Failures	69
3.5	Cooper-Harper Pilot Opinion Rating Scale	70
3.6	Summary of the Geometry, Weight, Drag Polar, and Performance Sizing Data for the Mega-Transport	71
3.7	Nondimensional Stability and Control Derivatives for the Mega-Transport	74
3.8	Longitudinal Transfer Functions for the Mega-Transport - Cruise Condition	77

## LIST OF TABLES (CON'T)

<u>Table</u>	<u>Title</u>	<u>Page</u>
3.9	Longitudinal Mode Flying Quality Parameters and Flying Quality Levels for the Mega-Transport - Cruise Condition	78
3.10	Longitudinal Transfer Functions for the Mega-Transport - Approach Condition	79
3.11	Longitudinal Mode Flying Quality Parameters and Flying Quality Levels for the Mega-Transport - Approach Condition	80
3.12	Lateral-Directional Transfer Functions for the Mega-Transport - Cruise Condition	81
3.13	Lateral-Directional Roll Performance Parameters and Flying Quality Levels for the Mega-Transport - Cruise Condition	83
3.14	Lateral-Directional Spiral and Dutch Roll Parameters and Flying Quality Levels for the Mega-Transport - Cruise Condition	84

## LIST OF TABLES (CON'T)

<u>Table</u>	<u>Title</u>	<u>Page</u>
3.15	Lateral-Directional Transfer Functions for the Mega-Transport - Approach Condition	85
3.16	Lateral-Directional Roll Performance Parameters and Flying Quality Levels for the Mega-Transport - Approach Condition	87
3.17	Lateral-Directional Spiral and Dutch Roll Parameters and Flying Quality Levels for the Mega-Transport - Approach Condition	88

## LIST OF FIGURES

<u>Figure</u>	<u>Title</u>	<u>Page</u>
1.1	The DC-10 Commercial Jet Transport	9
1.2	Landing Results, F-15 Simulation	10
1.3(a)	Boeing's 600 - 650-Passenger Transport Concept	11
1.3(b)	Airbus Industrie's 600-Passenger Transport Concept	11
1.3(c)	McDonnell-Douglas MD-12 511-Passenger Transport Concept	12
2.1	Dutch Roll Mode as Seen by an Outside Observer	40
2.2	Phugoid Mode as Seen by an Outside Observer	41
2.3	Effect of Speed on F-15 Flight and Simulation Maximum Pitch Rates (CAS Off)	42
2.4	Landing Difficulty Parameter (LDP) for F-15 Simulation Flown with Manual Throttles-Only Control (Trim Airspeed 170 knots)	42

## LIST OF FIGURES (CON'T)

<u>Figure</u>	<u>Title</u>	<u>Page</u>
2.5	The F-15 Air Superiority Fighter	43
2.6	The Lear 24 Executive Jet	43
2.7	The PA-30 Light, Twin-Engine Airplane	44
2.8	The B-720 Commercial Jet Transport	44
2.9	The B-727 Commercial Jet Transport	45
2.10	The MD-11 Commercial Jet Transport	45
2.11	Longitudinal Block Diagram - Flight Path Angle Control	46
2.12	Lateral-Directional Block Diagram - Bank Angle and Heading Control	46
2.13	Time History of Throttles-Only Manual Landing of the F-15 Simulation (Trim Airspeed 170 knots - Pilot Inexperienced with Manual Throttles-Only Control)	47

## LIST OF FIGURES (CON'T)

<u>Figure</u>	<u>Title</u>	<u>Page</u>
2.14	Time History of Augmented Throttles-Only Landing of the F-15 Simulation (Trim Airspeed 170 knots - Inexperienced Pilot's First Landing Using System)	48
3.1	NASA Dryden B-720 Simulation Cockpit	89
3.2	Time-History of B-720 Augmented Throttles-Only Control System Approach and Landing; 160 knots, No Flaps, Light Turbulence, 1,000 Foot Offset from Runway	90
3.3	Mission Profile of the Mega-Transport	91
3.4	A Preliminary Three-View of the Mega-Transport	92
3.5	Short-Period Frequency Requirements for the Mega-Transport - Cruise Condition	93
3.6	Short-Period Frequency Requirements for the Mega-Transport - Approach Condition	93

## LIST OF FIGURES (CON'T)

<u>Figure</u>	<u>Title</u>	<u>Page</u>
3.7	Minimum Dutch Roll Frequency and Damping Ratio Requirements for the Mega-Transport - Cruise Condition	94
3.8	Minimum Dutch Roll Frequency and Damping Ratio Requirements for the Mega-Transport - Approach Condition	94
3.9	Pilot/Engine/Airframe Closed Loop System	95
3.10	Measured Data with Fitted Pilot Model $H_p(\omega)$ for Disturbance Task	96



## CHAPTER 1

### INTRODUCTION

#### 1.1. DOUGLAS DC-10 UNITED AIRLINES ACCIDENT<sup>1,2,3,4,5,6</sup>

United Airlines Flight 232 from Denver to Chicago was cruising above Iowa at 37,000 feet on July 19, 1989. About one hour into the flight, the flight crew heard an explosion and the DC-10 (see Figure 1.1) began to shudder. The instruments showed that the tail-mounted engine had failed.

As the captain and the first officer struggled to control the aircraft, the flight engineer reported that all the hydraulic gauges were reading zero. There was no fluid and no pressure in any of the three independent hydraulic systems.

Primary flight controls on the DC-10 consist of inboard and outboard ailerons, two-section elevators, and a two-section rudder. Secondary flight controls consist of leading edge slats, spoilers, inboard and outboard flaps, and a dual-rate movable horizontal stabilizer. Flight control surfaces are segmented to achieve redundancy. Each primary and secondary control surface is powered by two of three independent hydraulic systems.

The three independent, continuously operating hydraulic systems are intended to provide power for full operation and control of the airplane in the event that one or two of the hydraulic systems are rendered inoperative. System integrity of at least one hydraulic system is required - fluid present and the ability to hold pressure -

for continued flight and landing. There are no provisions for reverting to manual flight control inputs.

Loss of hydraulic fluid in all three hydraulic systems made control of the aircraft using the flight control systems impossible. At this time the pilot declared an emergency. The aircraft was re-routed to Sioux City municipal airport due to the 8,999 foot long runway.

The passengers were told of the engine failure and the flight attendants were instructed to prepare the cabin for an emergency landing. Among the passengers was an off-duty United Airlines training check pilot, who had logged 3,000 of his 23,000 flight hours in DC-10s. He offered his help and was immediately invited up to the cockpit.

The check pilot was asked to go back into the cabin and inspect the wings. The inboard ailerons were displaced slightly upwards, the spoilers were locked down, and there was no movement of the flight control surfaces. The first officer would later perform a cabin check and report that, in addition, the horizontal stabilizers were badly damaged.

The captain directed the check pilot to take control of the throttles to free the captain and first officer to try once more to manipulate the flight controls. The check pilot attempted to use engine power to control pitch and roll. Control of the aircraft was extremely difficult. It took anywhere from 20 to 40 seconds after a thrust adjustment for the intended change in attitude to occur.

The pilots jettisoned as much fuel as possible and extended the landing gear by means of a backup system. The flight crew said that

they made visual contact with the airport about nine miles out. Though they had planned on landing on Runway 31 due to its length, the aircraft was lined up with shorter Runway 22. Because of the difficulty in making turns, the crew decided to land on Runway 22.

The check pilot worked the throttles continuously during final approach. The flaps and slats could not be extended since they operated using the hydraulic system. Visual cues and the first officer's airspeed indicator were used to determine the flight path and the need for thrust changes. The aircraft was fairly well aligned with the runway, but was descending at a high rate.

On final approach, the nose pitched down and the right wing dropped. First ground contact was made by the right wing tip followed by the right main landing gear. The airplane skidded to the right of the runway and rolled to an inverted position. The airplane cartwheeled and ignited in flame, coming to rest after crossing Runway 17.

Fire fighting and rescue operations began immediately, but the aircraft was destroyed by impact and fire. There were 296 passengers and crewmembers aboard Flight 232 - 185 of them survived the crash.

The FAA determined that the tail-mounted engine experienced an uncontained failure of the stage 1 fan rotor disk assembly. The engine fragments severed the Number 1 and Number 3 hydraulic system lines. In addition, the forces of the engine failure fractured the Number 2 hydraulic system, rendering the three hydraulic-powered flight control systems inoperative. Typical of all wide-body

transport aircraft, there are no alternate power sources for the flight control systems.

Because of the loss of the three hydraulic systems, the flight crew was confronted with a unique situation that left them with very limited control of the airplane. The only means available to fly the airplane was manipulation of thrust available from the remaining two wing-mounted engines. The primary task confronting the flight crew was controlling the flight path. This task was extremely difficult to accomplish because of the need to use the engine throttles asymmetrically to maintain lateral roll control coupled with the need to use increases and decreases in thrust to maintain pitch control. The flight crew found that despite their best efforts, they could not maintain a stabilized flight condition.

Douglas Aircraft Company, the FAA, and United Airlines considered the total loss of hydraulic-powered flight controls so remote that no procedure to counter such a situation was ever conceived. The simulator reenactment of the events leading to the crash landing revealed that landing under these conditions involves many variables that affect the extent of controllability during the approach and landing such as airspeed, ground effect, aircraft attitude, and rate of descent. While any one of these parameters might be controllable by the flight crew, it was virtually impossible to control all parameters simultaneously.

The National Transportation Safety Board concluded that the damaged DC-10 aircraft was marginally flyable using throttle controls to control the thrust on the remaining two engines. However, a safe landing on a runway was determined to be virtually

impossible with the loss of all hydraulic flight controls. The Safety Board ruled that under the circumstances, the United Airlines flight crew performance was highly commendable and greatly exceeded reasonable expectations.

## 1.2. NATIONAL TRANSPORTATION SAFETY BOARD RECOMMENDATIONS<sup>1</sup>

As a result of the United Airlines DC-10 accident at Sioux City, the National Transportation Safety Board reviewed alternate flight control system design concepts for wide-body airplanes. The concept of three independent hydraulic systems, as installed on the DC-10, is not unique. Boeing and Airbus have three such systems on some of their most recently certified models. Lockheed and Boeing have also provided four independent systems on some of their wide-body airplanes.

The Safety Board could find no inherent safety advantage to the installation of additional independent hydraulic systems for flight controls beyond those currently operating in today's fleet. However, the Safety Board believes that backup systems to the primary hydraulic systems should be developed and included in the initial design for certification. Such backup systems are particularly important for the coming generation of wide-body airplanes. Manual reversion flight control systems are quite likely impractical because of the power requirements to deflect large control surfaces that are heavily loaded. Therefore, the Safety Board recommended that the

FAA encourages continued research and development into backup flight control systems for newly certificated wide-body airplanes that employ an alternate source of motive power separate than that used for the conventional control system.

### 1.3. STUDIES REGARDING USE OF THROTTLES FOR EMERGENCY FLIGHT CONTROL<sup>7,8,9</sup>

The NASA Dryden Flight Research Facility (NASA Dryden) at Edwards Air Force Base, California, has been the site for conducting preliminary flight, ground simulator, and analytical studies regarding the use of throttles for emergency flight control of a multi-engine aircraft. This investigation was begun as a result of the relatively successful attempted landing of the United Airlines DC-10 at Sioux City. The objective has been to determine the degree of control power available with the throttles for various classes of airplanes and to investigate the development of possible control modes for future airplanes.

The research work performed thus far at NASA Dryden appears to indicate that control of an aircraft with partial or total flight control system failure using throttles-only control is feasible. Based on simulator and flight results, all of the airplanes studied at NASA Dryden to date have exhibited some control capability with throttles-only control. All airplanes could be controlled in a gross manner, although it was very difficult to achieve precise control with

manual throttle control. Landings using manual throttles-only control were extremely difficult.

As a result of these studies, an augmented control system has been developed at NASA Dryden. The control mode uses pilot stick inputs, with appropriate gains and feedback parameters, to drive the throttles. Performance in the augmented mode was greatly improved. Figure 1.2 shows the F-15 simulation landing results for the manual throttles-only mode and for the augmented throttles-only mode. The distance from the runway centerline, distance from the runway threshold, and sink rate and roll angle are plotted in a three-dimensional representation. As is graphically demonstrated, the augmented throttles-only control mode resulted in safe and survivable landings, whereas the manual throttles-only control mode resulted primarily in nonsurvivable crashes. Based on simulation results, it appears that the augmented control system makes runway landings practical using throttles-only control.

#### 1.4. PURPOSE AND OBJECTIVES<sup>10,11,12,13,14,15,16,17</sup>

Boeing, Airbus, and McDonnell-Douglas are currently in the preliminary phase of designing an ultra-high capacity jet transport consisting of 600 - 1,000 passengers (see Figure 1.3). The possibility that one of these large transports might crash due to total failure of the flight control system is not unthinkable, particularly in light of the Sioux City accident. In view of the work already done at NASA Dryden, it seems reasonable to ask the following questions:

- Is it possible to arrange the engines in a large passenger transport in such a way that flight path control using only the engines is not only possible, but meets Level 1 or Level 2 handling quality requirements?

- Since total failure of the primary flight control system can be caused by the failure of an engine, can the number of engines and their arrangement be selected such that flight path control with one engine inoperative is still possible with Level 1 or Level 2 handling quality requirements?

- Can one or more levels of primary flight control system redundancy be eliminated in an airplane equipped with a Level 1 or Level 2 engine control system, allowing the engine thrust to be used as a backup flight control system?

- What are the weight, drag, systems design, and cost benefits associated with such a design?

This comprehensive proposal will present a procedure which will attempt to answer these important questions. Chapter 2 contains the background information pertinent to this proposal, while Chapter 3 presents an outline of the proposed work.



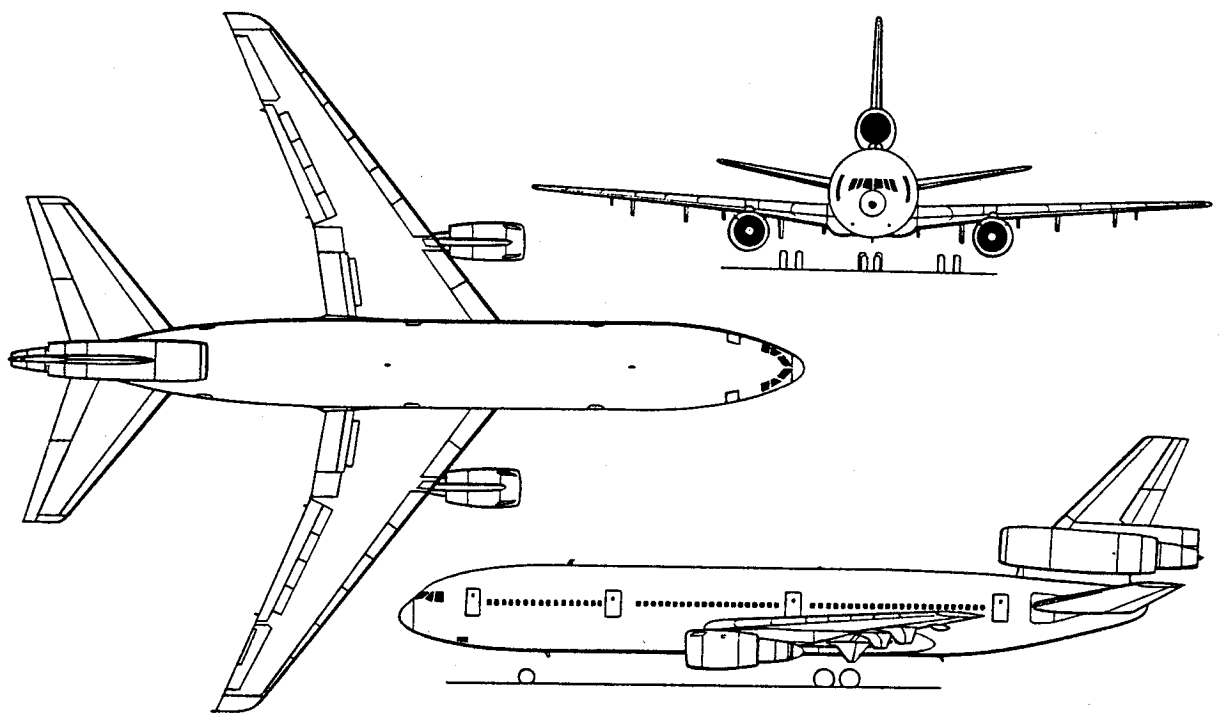


Figure 1.1 The DC-10 Commercial Jet Transport (Ref. 5)

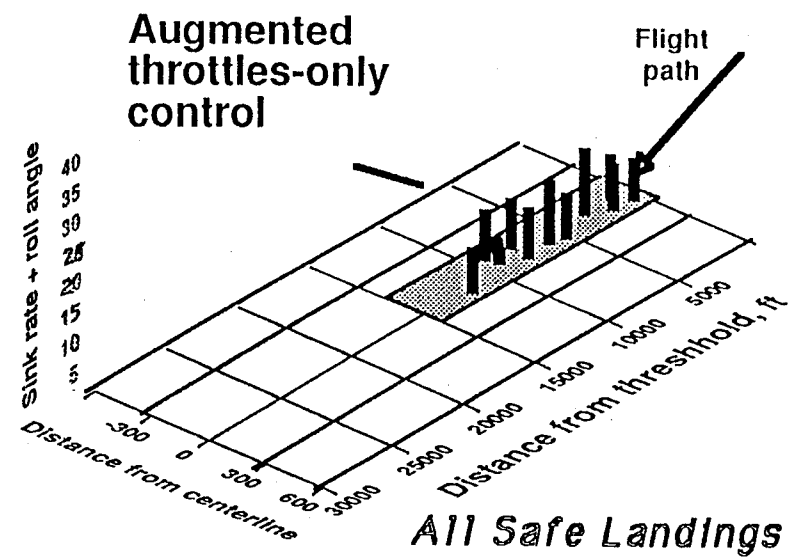
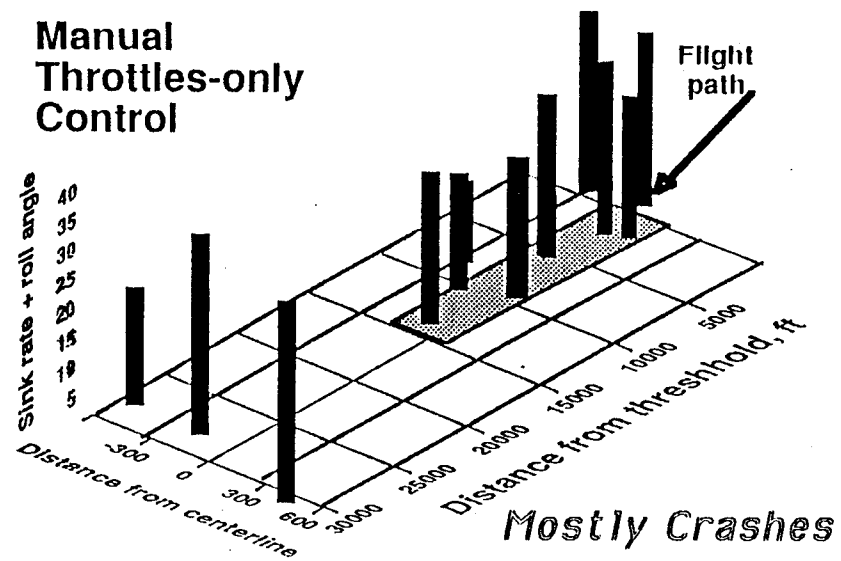


Figure 1.2 Landing Results, F-15 Simulation (Refs. 18 and 19)

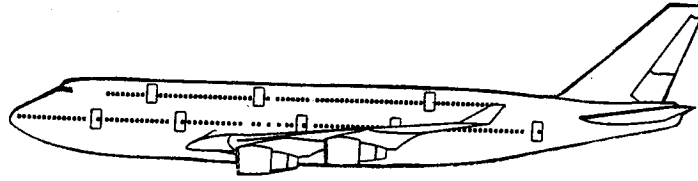


Figure 1.3(a) Boeing's 600 - 650-Passenger Transport  
Concept (Ref. 11)

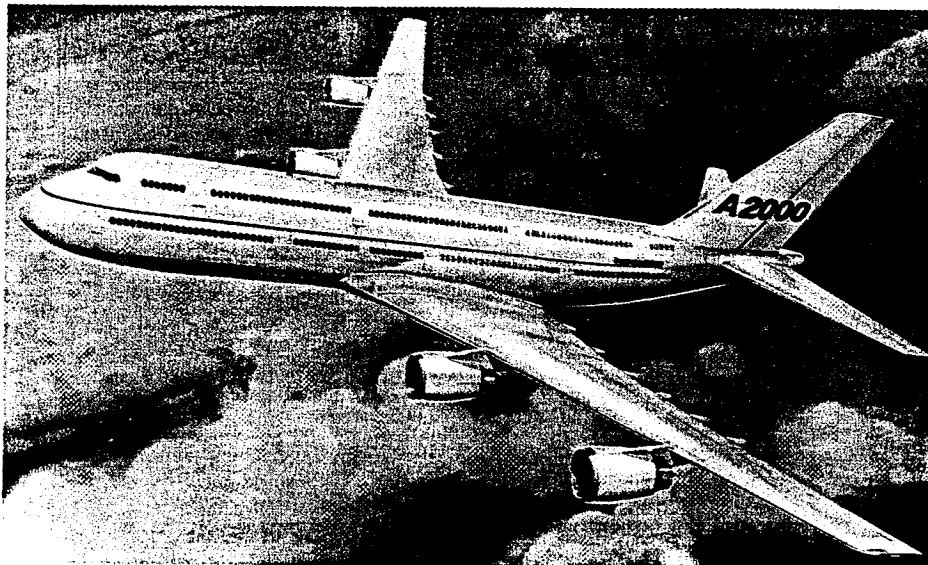


Figure 1.3(b) Airbus Industrie's 600-Passenger Transport  
Concept (Ref. 10)

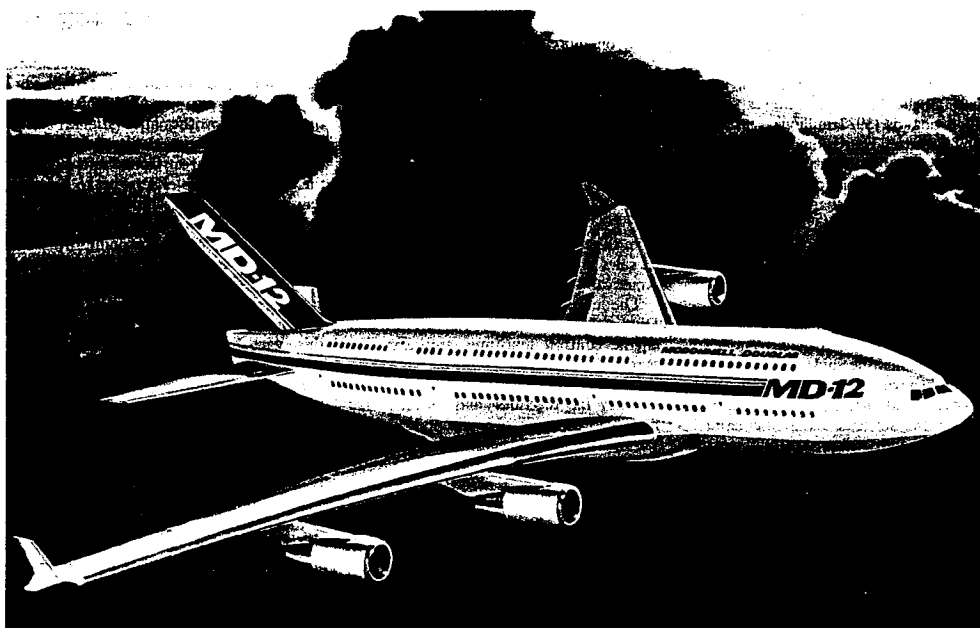


Figure 1.3(c) McDonnell-Douglas MD-12 511-Passenger Transport  
Concept (Ref. 15)

## CHAPTER 2

### BACKGROUND INFORMATION

#### 2.1. INTRODUCTION<sup>1,9</sup>

Steady level cruise flight is attained when the forces acting on the airplane are in a state of equilibrium; that is, thrust equals drag and the weight of the airplane is balanced by the lift forces produced primarily by the wing and horizontal stabilizer. Lift, drag, and thrust vary with airspeed, angle of attack, and atmospheric conditions.

Transient changes from the steady cruise condition are achieved by manipulating the cockpit controls to move the longitudinal controls (stabilizer, elevator, canard, or canardvator) or the lateral-directional controls (aileron, spoiler, differential stabilizer, or rudder). The deflection of the longitudinal control surface causes a change in the attitude, angle of attack, and airspeed of the aircraft. In routine flight, the pilot will change both thrust and longitudinal control surface position to attain a new steady flight path. Lateral-directional control is normally achieved by using the lateral-directional control surfaces to produce a bank angle that will result in a turn or change in the direction of the flight heading.

An inability to reposition the control surfaces severely restricts the pilot's control over such flight path and heading changes by eliminating the essential means of changing the normal force balance. Flight control systems are one of the most crucial systems on an aircraft.

Current generation aircraft rely on multiple, independent flight control systems so that any single failure of an aircraft component will not disable more than one system, thus leaving the aircraft with satisfactory flight control capability. Despite these design objectives, failures have occurred where aerodynamic control surface effectiveness has been significantly impaired or completely lost. This can result from impairment and failures in the electrical, hydraulic, and hardware systems. Such problems can be the result of internal aircraft system failures (due to engine failure, fatigue, corrosion, improperly executed repairs, or terrorist damage) or external damage (due to bird strikes, mid-air collision, or tactical battle damage). In such cases, throttles can be used as the primary means of controlling the aircraft. Several examples will be described in the following section.

## 2.2. AIRCRAFT INCIDENTS WITH SIGNIFICANT FLIGHT CONTROL FAILURES

The DC-10 accident in Sioux City, Iowa, was not an isolated incident regarding the loss of the flight control system. Significant flight control failures have been documented in at least five other recent incidents. These incidents are described in detail in the following subsections.

### 2.2.1. Douglas DC-10 American Airlines Incident<sup>20</sup>

On June 12, 1972, American Airlines Flight 96 took off for Buffalo from Detroit with 57 passengers and 10 crew members on board. Approximately 10 minutes into the flight, the aft left cargo door separated from the aircraft, causing cargo compartment decompression.

When the door separated, a section of the aft coach lounge floor 6 - 8 feet square on the left side of the cabin broke loose from the support frames and dropped part way into the cargo bay. Part of the right side floor buckled to a lesser degree. There were no passengers seated there.

The only sign of an abnormal condition initially was a swirl of dust and debris in the cockpit and in the cabin, the pilot reported. Then the aircraft entered a slight right yaw as a result of the severing of several control cables when the aft cabin floor buckled. The control cables which were severed were the rudder control cables, except for those controlling the rudder trim system, the left elevator control and stabilizer trim, and the power control and fuel shutoff cables for the tail-mounted engine.

Both sections of the rudder and the left elevator went into trail position and the tail engine went to idle power. The pilot reported no unusual attitude changes except for a slight right yaw. There were no significant difficulties in controlling the aircraft during flight. Ailerons alone appeared to provide enough directional control.

Controlling the aircraft after touchdown was more difficult. The flight crew used spoilers and differential reverse thrust on the

two wing-mounted engines to steer and stop the aircraft. Minor injuries were suffered by nine passengers in the escape chute evacuation of the aircraft on the ground, but none were hospitalized.

#### 2.2.2. Douglas DC-10 Turkish Airlines Accident<sup>21,22</sup>

A Turkish Airlines DC-10 took off from Paris to London with 335 passengers and 11 crew members aboard on March 3, 1974. Approximately 9 minutes after takeoff, the aft left cargo door separated while the aircraft was at 12,000 feet and cruising at 300 knots. Cabin depressurization followed separation of the door.

The aircraft went into a pronounced nose-down attitude, power was reduced, and a roll to the left began. Accident investigators determined that the DC-10 hit the ground at 420 knots and with the left wing down. A swath more than 3,000 feet long had been cut through the forest where the aircraft struck. The aircraft literally disintegrated as it plowed through the trees, killing all on board.

It was assumed that when the cabin depressurized, the cabin floor buckled, severing the hydraulic lines and control cables in a manner similar to that of the American Airlines incident in 1972. When the hydraulic lines were severed, the hydraulic-powered flight control systems were rendered inoperative.

#### 2.2.3. Lockheed C-5A USAF Accident<sup>23,24</sup>

April 4, 1975, a USAF/C-5A took off from an airfield in Viet Nam with 178 persons, mostly Vietnamese orphans, aboard. The



aircraft was passing through 23,000 feet and was about 5 miles offshore en route to Clark air base in the Philippines when the rear pressure bulkhead, which is part of the cargo-loading ramp, failed. This failure caused the complete loss of the primary and secondary hydraulic systems, loss of cabin pressurization, and secondary damage to the aft fuselage.

Loss of both the hydraulic systems caused the crew to lose rudder, elevator, and flap control. The aircraft remained roughly in trim and was maneuvered using ailerons and throttle controls. The crew commented on the difficulty in achieving precise control due to the slow response of the engines. They practiced using this control mode for 30 minutes, made a practice landing at 10,000 feet, then tried an approach to the runway.

About 7 miles from the airport at 5,000 feet and aligned with the runway, the crew lowered the landing gear and at about the same time the aircraft's rate of descent increased excessively. The aircraft hit very hard about 1.5 miles short of the runway, broke up, and was destroyed by fire. There were no survivors.

#### 2.2.4. Lockheed L-1011 Delta Airlines Incident<sup>25</sup>

Near midnight, April 12, 1977, Delta Airlines Flight 1080 prepared to depart San Diego for a flight to Los Angeles. During taxi out, a flight control check of the stabilizer, ailerons, and spoilers was made. The proper response was verified by the surface position indicators and by the normal 'feel' of the wheel.

During takeoff acceleration, the L-1011 lifted off with little or no control input and a zero stick force. Immediately after liftoff, an abrupt nose-high excursion in pitch and a roll to the left was experienced that was controllable, although the pilot did hit the full forward limit of the control column during the abrupt pitch-up.

At an altitude of approximately 400 feet and an airspeed of 170 knots, the pitch exceeded 18 degrees. The aircraft was trimmed with full nose-down stabilizer trim, but no change in the pitch attitude was observed. The aircraft continued to pitch up and climb as the airspeed decayed. In addition, the pilot continually fought a tendency of the aircraft to maintain a left-bank attitude.

Pitch attitude exceeded 22 degrees and the airspeed fell to 138 knots when the pilot felt that loss of the aircraft due to stall was eminent. If pitch could be reduced, airspeed would be regained and some degree of controllability might be obtained.

The pilot abruptly reduced thrust on all three engines and recognized a change in control 'feel'. The airspeed increased as the pitch angle dropped. Increased thrust on the left engine was implemented to compensate for the left-roll tendency. One inch of control stick movement was now available to the pilot.

The L-1011 was controlled during flight by using the throttles as the primary flight control system. The approach was set up and a successful landing was made. Upon touchdown, the pilot found that the nose did not come down even with the control column full-forward. It was necessary to apply main-wheel braking to force the nose wheel down.

Upon examination of the aircraft, the malfunction was determined to be the left elevator jammed in a 19 degree nose-up attitude. Presumably the left elevator aft drive quadrant and drive cable failed during the flight control check prior to takeoff. There is no cockpit indication for this type of failure on the L-1011.

#### 2.2.5. Boeing 747 Japan Airlines Accident<sup>26,27,28,29,30,31</sup>

August 12, 1985, Japan Airlines Flight 123 took off from Tokyo's Haneda Airport bound for Osaka. At an altitude of 24,000 feet, an impact force occurred which raised the nose of the 747 aircraft. Immediately after the impact force, hydraulic pressure dropped and rudders, ailerons, elevators, and yaw dampers became inoperative. Significant altitude and speed changes and roll oscillations occurred. The aircraft rolled +/-40 degrees and altitude and speed changed by +/-1,500 feet and +/-25 knots, respectively.

The flight crew attempted to fly the aircraft using only throttle controls for approximately 30 minutes. The pilot radioed that he was unable to control the aircraft immediately before the aircraft crashed into a mountainside 51 miles from Tokyo. The 747 had 520 passengers aboard. There were only 4 survivors.

Upon examination of the wreckage, it was believed that the impact force was a ruptured aft bulkhead. When the bulkhead ruptured, the rudders, part of the vertical stabilizer, and most of the tail cone separated from the fuselage while the aircraft was in flight. All four hydraulic lines, which run into the tail cone, were severed

when the tail cone separated, rendering all control surfaces inoperable.

## 2.3 PRINCIPLES OF ENGINES-ONLY CONTROL

The aircraft incidents described in Section 2.2 all experienced partial or total flight control system failure and all exhibited an ability to use engine thrust for emergency control. Engine thrust can be used to control the heading and flight path of a multi-engine airplane. This section presents the principles of engine-only flight control.

### 2.3.1. Yaw-Roll Control<sup>7,18,32,33</sup>

Differential thrust, a difference in thrust between the engines on the right side of the fuselage and the left side of the fuselage, generates sideslip. Through the normal dihedral effect present on most airplanes, this results in roll. Roll from differential thrust is controlled to establish a bank angle, which results in a turn and a change in aircraft heading.

Some aircraft will exhibit a coupled mode between roll and yaw called dutch roll. The dutch roll mode consists of a lightly damped, moderately low frequency oscillation. An example of what a complete three-degrees-of-freedom dutch roll motion looks like to an outside observer is shown in Figure 2.1.

Controlling dutch roll using throttles alone can cause roll and heading control difficulties for the pilot. The dutch roll frequency during low altitude cruise flight for a Boeing 747 aircraft is 1.05 radians/second. The control system time delay in response to throttles is approximately one second. During that one second, the 747 has completed 1.05 radians, or 60 degrees, of the dutch roll cycle. Therefore, there is a 60 degree phase lag that the pilot must attempt to anticipate. The F-15 fighter aircraft, during low altitude slow flight, has an even larger 112 degree phase lag in the dutch roll.

### 2.3.2. Pitch Control<sup>7,18</sup>

Pitch control caused by throttle changes is more complex. The desired result is to stabilize and control the vertical flight path. There are several effects that may be present which are described in the following subsections. One of these effects may dominate, depending on the aircraft characteristics and flight conditions.

#### 2.3.2.1. Phugoid Oscillations<sup>1,7,18,32</sup>

The airplane will continuously seek the airspeed and flight path angle at which the forces balance for the existing longitudinal control surface position and the existing thrust level. This produces an approximately constant angle of attack motion in which kinetic and potential energies (airspeed and altitude) are traded. This longitudinal oscillation is called the phugoid mode. An example of

what the phugoid motion looks like to an outside observer is shown in Figure 2.2.

The phugoid produces a long period of pitch oscillation and will produce speed variations about the trim speed. If the speed varies from the trim speed, the airplane will change pitch and either climb or descend to recover to the trim speed. For example, if the speed falls below the trim speed while the airplane is in level flight, the lift produced by the wing is not sufficient to maintain altitude. The airplane will start to descend and pick up speed. Normally, the airspeed will increase beyond the trim speed and the airplane lift will become greater than required, resulting in an increase in vertical velocity and subsequent climb. During the climb, the airspeed will fall toward the trim speed and the cycle continues.

The time to complete one oscillation is called the period of the phugoid. The period of the phugoid is directly proportional to the forward velocity and is typically about one minute for large jet transports, but may be as long as several minutes for some airplanes. The period is a function primarily of speed and not of aircraft design.

Whenever elevator control is present, the phugoid is easily damped and is not noticeable to the pilot. In a situation involving control surface failure, however, the control surfaces are 'frozen' at the time of failure and, therefore, the trim speed is set. Phugoid damping becomes a critical factor during approach and landing. A landing which occurs on the down slope of the phugoid sinusoidal curve will have an extremely high rate of descent.

Properly sized and timed throttle inputs to control pitch can be used to damp unwanted phugoid oscillations, but the phugoid is

difficult to damp with changes in thrust alone without prior experience flying throttles-only flight control. One reason for this difficulty is that pitch rate, shown in Figure 2.3, is a function of both speed and of whether the throttles are being commanded to go from high thrust to lower thrust, or from low thrust to higher thrust. The low pitch-down capability relative to the pitch-up capability is because the throttle setting for power for level flight (PLF) is much closer to idle than to intermediate.

Techniques for finding the proper degree of throttle input to make a survivable landing were learned after approximately five landings for the F-15 fighter, as can be seen in Figure 2.4. These techniques will vary depending on the aircraft, engine response for a transport being different from that of a fighter.

#### 2.3.2.2. Flight Path Angle Change Resulting from Speed Stability<sup>7,18</sup>

Most airplanes exhibit positive speed stability. An increase in thrust will create a speed increase which, in turn, causes an increase in lift. This produces an increase in the flight path angle. The flight path angle will increase for about 10 seconds. During this time, the airplane climbs, the airspeed will fall toward the trim speed, and phugoid oscillations will be initiated. The degree of speed stability is affected by aircraft configuration and the center of gravity (c.g.) location.

#### 2.3.2.3. Pitching Moment Resulting from Thrust Line Offset<sup>7,18</sup>

If the engine thrust line does not pass through the c.g., there will be a pitching moment introduced by thrust change. For many transport aircraft, the thrust line is below the c.g. Increasing thrust results in a nose-up pitching moment, with the magnitude being a linear function of the thrust change. This is the desirable geometry for throttles-only control, because a thrust change immediately starts the nose in the same direction needed for the long-term flight path angle change. High-mounted engines result in this effect fighting the speed stability effects. The pitching moment caused by the thrust will cause a change in the trimmed angle of attack and airspeed as well as changing the long-term flight path angle.

#### 2.3.2.4. Flight Path Angle Change Resulting from the Vertical Component of Thrust<sup>7,18</sup>

If the thrust line is inclined to the flight path, an increase in thrust will cause a direct increase in vertical velocity, that is, rate of climb. For a given aircraft configuration, this effect will increase as angle of attack increases.

#### 2.3.3. Speed Control<sup>7,18</sup>

Once the flight control surfaces become locked at a given position, the trim airspeed of most airplanes is affected only slightly by engine thrust. Retrimming to a different speed may be achieved



by other techniques. These techniques include moving the c.g., lowering the flaps and landing gear, and by using stabilizer trim, if available. In general, the speed will need to be reduced to an acceptable landing speed, implying the need to develop nose-up pitching moments. Methods for accomplishing this include moving the c.g. aft and selective lowering of flaps. In aircraft with more than two engines, speed can be reduced by increasing the thrust of low-mounted engines. The retrimming capability varies widely between airplanes.

#### 2.3.4. Thrust Response<sup>7,18</sup>

Most turbine engines respond faster at higher thrust levels than at lower thrust levels. High-bypass turbofans are particularly slow to respond at flight idle. A high-bypass ratio engine takes as long as three seconds to go from flight idle to 30 percent thrust, then three more seconds to go from 30 to 100 percent thrust. Turbojet and low-bypass ratio turbofan engines typical of fighter airplanes and older transports are faster in response, in some cases as fast as 2.5 seconds from idle to full thrust.

#### 2.3.5. Effects of Speed on Propulsive Control Power<sup>7,18</sup>

For turbine-powered airplanes, engine thrust is not a strong function of airspeed. However, the stabilizing effects of vertical and horizontal stabilizers are a function of dynamic pressure, which is

proportional to the square of the airspeed. Consequently, the propulsion system control power increases as airspeed decreases. For example, at high airspeed differential thrust develops a yawing moment that is small compared to the restoring moment produced by the vertical tail. Therefore, the sideslip is small and the roll rate resulting from differential thrust is low. At low speed, the differential thrust moment may be the same as at high speed. The aerodynamic restoring moment will be much smaller and larger sideslip will develop, producing higher roll rates. A similar effect occurs in the pitch axis, where speed stability increases as speed decreases.

#### 2.4. HISTORICAL REVIEW<sup>7,8,18</sup>

The NASA Dryden Flight Research Facility (NASA Dryden) at Edwards Air Force Base, California, has been the site for conducting preliminary flight, ground simulator, and analytical studies regarding the use of throttles for emergency flight control of a multi-engine aircraft. This investigation was begun by Frank W. Burcham, Jr., chief of NASA Dryden's propulsion and performance branch, as a result of the relatively successful attempted landing of the United Airlines DC-10 at Sioux City, Iowa, in July 1989. The objective has been to determine the degree of control power available with the throttles for various classes of airplanes and to investigate the development of possible control modes for future airplanes.

Several airplanes, including a light twin-engine piston-powered airplane, jet transports, and a high performance fighter were studied during flight and piloted simulations. Simulation studies used the B-720, B-727, MD-11, and F-15 aircraft. Flight studies used the Lear 24, Piper PA-30, and F-15 airplanes. Some physical characteristics of these airplanes are given in Table 2.1.

#### 2.4.1. Flight Research Studies

Some preliminary flight research studies were conducted on three airplanes: the F-15, the Lear 24, and the PA-30 aircraft.

##### 2.4.1.1. F-15 Air Superiority Fighter<sup>7,18</sup>

The F-15 airplane (see Figure 2.5) is a high performance fighter with a maximum speed of Mach 2.5. It has a high wing with 45 degrees of leading-edge sweep and twin vertical tails. It is powered by two F100 afterburning turbofan engines mounted close together in the aft fuselage. The thrust-to-weight ratio is very high, approaching one at low altitudes. The engine response is fast - 3 seconds from idle to intermediate power. The F-15 has a mechanical flight control system augmented with a high-authority electronic control augmentation system. Hydraulic power is required for all flight control surfaces.

In flight tests using the NASA F-15 airplane, three pilots evaluated the controllability of the F-15 airplane with throttles only, leaving the stick and rudder centered. Using only manual throttle

control, pilots could roll the airplane, hold a bank angle, and hold an assigned heading.

If the airplane was trimmed at 170 knots, adequate pitch control was available to hold altitude within approximately 100 feet. If a flight control failure occurred at higher speeds, some method would be necessary to retrim the F-15 to lower speeds. Use of fuel transfer to move the c.g. aft would be one way to develop nose-up pitching moments, which would slow the F-15. The ramps of the variable capture inlets are also useful in generating nose-up moments. Extension of the landing gear results in almost no change in speed on the F-15 airplane.

#### 2.4.1.2. Lear 24 Executive Jet Transport<sup>7,18</sup>

The Lear 24 airplane (see Figure 2.6) is a twin-engine business jet. The low-mounted wing has 13 degrees of sweep. The engines, GE CJ610 turbojets with 2,900 pounds of thrust each, are mounted high on the aft fuselage. The airplane has a T-tail arrangement. Maximum weight is 11,800 pounds. The Lear 24 has a thrust-to-weight ratio of approximately 0.5. The turbojet engines respond rapidly to throttle changes, 2.5 seconds from idle to full thrust.

The airplane used in this evaluation was the Calspan variable stability airplane. It is equipped with the basic Lear 24 mechanical control system, including an electric stabilizer pitch trim capability. In addition, there are hydraulic actuators that add electric inputs from the variable stability system to the mechanical system.

The Lear 24 characteristics with throttles-only control were investigated at a speed of approximately 200 knots. Roll control power is quite large. The basic Lear 24 pitch control capability was also investigated. In contrast to the roll axis, pitch control with thrust was very difficult. Because of the high engine placement, a thrust increase caused a nose-down pitch. Eventually, the speed stability would bring the nose back up. The phugoid was very difficult to damp with throttle inputs. Despite these difficulties, the Lear 24 was flown for 20 minutes using only the throttles. Roll and heading were controlled precisely and altitude was maintained within 500 feet.

#### 2.4.1.3. PA-30 Piston-Powered Light Twin-Engine Plane<sup>7,18</sup>

The Piper PA-30 airplane (see Figure 2.7) is a light, twin-engine, four-place airplane. It has a low-mounted unswept wing, and the engines are mounted ahead of the wing in nacelles. Maximum weight is 3,600 pounds. The engines are the Lycoming IO-320 model, rated at 160 horsepower each.

The PA-30 was flown with throttles only and it had significant control power. The roll control on the PA-30 is highly nonlinear. It appears that the major rolling moment is caused by reducing the throttle on one side until the blowing over the wing is sharply reduced. The linear response to differential thrust seen on other jet-powered airplanes was not present. Pitch control is difficult. There is adequate control power available from speed stability, but the longitudinal phugoid is hard to damp. Overall, it was possible to

maintain gross control of heading and altitude, but landing on a runway would be extremely difficult.

#### 2.4.2. Simulator Studies

Piloted simulator studies of engines-only flight control capability were conducted on the B-720, B-727, MD-11, and the F-15 aircraft. One task evaluated was 'up-and-away' control. This is the ability to control heading to within a few degrees, and to control altitude to within +/- 200 feet. The other task was landing on a runway.

##### 2.4.2.1. B-720 Commercial Jet Transport<sup>7,18</sup>

The Boeing 720 airplane (see Figure 2.8) is a four-engine transport designed in the late 1950's. It has a 35 degree swept wing mounted low on the fuselage, the four engines mounted on pods below and ahead of the wing. The engines are Pratt and Whitney JT3C-6 turbojets. The airplane is equipped with a conventional flight control system incorporating control cables and hydraulic boost. It also incorporates a slow-rate electric stabilizer trim system. The flaps are electrically controlled.

The pilot of the B-720 simulation flew manually using the throttles only. Good roll capability was evident. Good pitch capability was also found, with some pitching moment caused by the thrust line being below the c.g., and some pitching moment caused by speed stability.

It was possible for a pilot to maintain gross control, hold heading and altitude, and make a controlled descent. However, it was extremely difficult for a pilot to make a landing on a runway. There was a one second lag in pitch and roll before the airplane began to respond to the throttles. Judging the phugoid damping was difficult, and the lightly damped dutch roll was a major problem in roll and heading control. Although a few pilots did develop techniques for successful landings using manual throttles, most were unable to make repeatable successful landings.

#### 2.4.2.2. B-727 Commercial Jet Transport<sup>7,18</sup>

The Boeing 727 three-engine transport (see Figure 2.9) has a swept wing and a T-tail. The three Pratt and Whitney low-bypass ratio turbofan engines are mounted in the aft fuselage. The two outboard engines are mounted on short pylons, while the center engine is located in the aft fuselage and has an inlet above the fuselage. The engine response was slow from idle to an engine pressure ratio of 1.2, then fast until full thrust was reached.

Pitch control power was evaluated. There is significant pitching authority with thrust on the B-727. The roll capability, while much less than the F-15 or B-720 airplanes, was surprisingly large considering the fuselage-mounting of the engines.

The airplane was flown using differential engine thrust for bank angle and electric stabilizer trim in pitch, and gross control was possible. Precise control of the flight path angle using throttles was more difficult, however. Landings were attempted using differential

throttle and electric trim. Neither of the evaluation pilots could successfully land the airplane on the runway by themselves. The low roll rate and roll control lag made it nearly impossible to remain lined up with the runway.

Improved roll control was achieved by reducing the center engine throttle to idle; the higher thrust and the faster thrust response of the outboard engines improved directional control. Splitting the control task between two pilots also helped. One pilot would fly pitch with electric trim, while the other pilot used differential throttles for roll and heading control. Even with this technique, it was not possible to make consistent landings on the runway.

#### 2.4.2.3. F-15 Air Superiority Fighter<sup>7,18</sup>

A simulator study was performed on the NASA F-15 airplane. It was flown in a simulator cockpit with actual F-15 stick and throttles. A visual scene, including the Edwards dry lake bed runways, was provided on a video monitor.

The piloted F-15 simulation was used in a landing study. The pilots used throttles-only control to fly approaches and landings using the video display of the 15,000 foot-long Edwards Runway 22. During the initial landing attempts, control was extremely difficult. The phugoid mode was excited close to the ground and was a constant problem throughout touchdown. Throttle inputs to damp the phugoid were hard to judge. Roll control, while adequate in rate, had a troublesome one second lag. Most landings had such a high



sink rate that they were categorized in the 'certain damage' category; many were not survivable landings.

#### 2.4.2.4. MD-11 Commercial Jet Transport<sup>7,18,34</sup>

The MD-11 airplane (see Figure 2.10) is a large, long-range commercial transport. It has a 35 degree sweep, low-mounted wing. It is powered by three high-bypass turbofan engines, two mounted in underwing pods and the third mounted in the base of the vertical tail. The engines are slow to respond at low thrust levels, but respond well above 30 percent thrust.

Initial simulator results showed that up-and-away flight was possible - altitude could be maintained and heading could be held within reasonable limits. The low roll rate of the MD-11 made runway lineup very difficult, however, when landings were attempted in the simulator. While it was possible to come close to the runway, it was not possible to make repeatable controlled landings on the runway.

Later MD-11 simulator results with higher fidelity models showed that roll rates were higher than previously thought and that, with practice, manual landings were possible. These results were substantiated with flight data.

#### 2.4.3. Overall Flying Qualities<sup>7,18</sup>

Based on simulator and flight results, all the airplanes exhibited some control capability with throttles. All airplanes could

be controlled in a gross manner (heading and altitude could be maintained) although pilot workload was very high. Because of the phugoid characteristics and the lag associated with the engine thrust response, it was very difficult to achieve precise control with manual throttle control. Landings using manual throttles-only control were extremely difficult; landing at a predetermined point and airspeed on a runway was a highly random event.

#### 2.4.3.1. Augmented Control System<sup>7,9,18</sup>

An augmented control system was developed by Glenn B. Gilyard and Joseph L. Conley, both engineers at NASA Dryden, for the B-720 simulation. The control mode uses pilot stick inputs, with appropriate gains and feedback parameters, to drive the throttles.

In the pitch axis, a flight path angle command loop was implemented. The command is designed to act through the forward and aft motion of the stick and have a command capability of  $\pm 10$  degrees of flight path angle. In addition to flight path angle feedback, pitch rate is also fed back to augment the damping (see Figure 2.11).

The control for the roll axis was mechanized using differential throttle to command yaw, and hence, through dihedral effect, roll. Bank angle was commanded by lateral stick position. The damping of the augmented dutch roll mode is very light despite roll rate and sideslip feedback (see Figure 2.12). However, the mean bank angle holds well if care is taken not to excite the dutch roll. A study of lateral stick commanding only differential throttle (without any

feedback) was also conducted. The dutch roll damping problem was significantly reduced. However, there was a spiral instability to manually control.

Using the augmented control mode, it was possible for a pilot to make successful landings. Pilot proficiency improved rapidly with time, as the lead time required to compensate for slow engine response was learned. Landings without turbulence or with light turbulence were generally good. With moderate turbulence, pilot ratings degraded, but most landings were still successful.

The augmented mode developed for the B-720 airplane was incorporated into the F-15 simulator. Gain changes were made to account for the differences in throttle range and thrust, but the basic control concept remained the same. All the roll feedback gains were set to zero, making the lateral stick command differential thrust directly.

Performance of the F-15 in the augmented mode was greatly improved. Figure 2.13 demonstrates the time history of a throttles-only manual landing of the F-15 simulation. As can be seen from the figure, the pilot landed well short and to the right of the runway with a rate of sink of 20 feet per second. Figure 2.14 demonstrates the time history of an augmented throttles-only landing of the F-15 simulation. The rate of sink was well-controlled and the landing was on the center line of the runway.

As further testing was done on evaluating pilot performance while flying the augmented mode simulation, suggestions were made by some of the pilots to develop thumbwheel controllers to command bank angle and pitch attitude directly. The augmented mode aircraft

performance was sluggish and slow to respond compared with the baseline unaffected aircraft which the pilots were used to flying. Several pilots had some difficulty in flying the augmented mode with the control stick due to overcompensation and pilot induced oscillation (PIO) tendencies.

Currently, both methods of flying the augmented mode are available in the simulator. The advantage of the control stick is that it enables the pilot to control the disabled aircraft with conventional control methods (moving the stick forward and aft to control pitch and from side to side to control roll). The advantages of the thumbwheel are:

- reminds the pilot that the system is a slow-response, low-authority system
- good resolution (incremental commands are easily attained)
- the pilot is not required to hold the thumbwheel to maintain command (thumbwheels remain where set)
- separate thumbwheels for pitch and roll control (the control stick has virtually no pitch/roll isolation) and
- similar controls are used in transport aircraft to command the autopilot.

Further evaluation of pilot preference and performance is currently being researched.

The augmented control provided two important improvements over manual throttles-only control. First, the augmented control system used conventional flight control effectors such as a stick or autopilot pitch and bank angle control knobs, rather than the throttles. Second, feedback of key pitch and roll parameters was

provided to stabilize the flight path. In the pitch axis, flight path angle and pitch rate feedback are provided. The pitch rate feedback provides phugoid damping. In the roll axis, bank angle feedback was used for roll control.

By using the augmented system, precise control capability was greatly enhanced. The augmented modes effectively damped the phugoid and improved the roll characteristics. With the augmented system, it was possible to make repeatable landings on a runway and inexperienced pilots were able to make good landings on their first tries as was seen in Figure 2.14. Based on simulation results, it appears that the augmented control system makes runway landings practical using throttles-only control.

## 2.5. CURRENT RESEARCH<sup>19,35,36</sup>

Douglas Aircraft Company (DAC), in conjunction with NASA Dryden, is currently performing an evaluation of the augmented throttles-only control concept for the MD-11 on their MD-11 Flight Deck Simulator. In addition to the simulator studies, manual throttles-only control was flown on an actual MD-11 aircraft in September 1992. Although no throttles-only landings were attempted, an approach was made within 70 feet above the runway. The preliminary evaluation by both DAC and NASA pilots is that the results are "very promising".

In addition to the work being done on the MD-11, an augmented propulsion controlled aircraft (PCA) system has been

designed for the NASA F-15. On February 5, 1993, the F-15 was flown within 10 feet above the runway under PCA control. Sink rate was well within acceptable limits and bank angle was less than one degree. There have been nine PCA flights to date with additional flights planned for March 1993. The F-15 has been flown in PCA mode at different fuel weights, different speeds, and different attitudes. These flight data are currently being analyzed before the next flights in March. On the basis of on initial flight test results, an augmented throttles-only control system shows promise of making repeatable runway landings of the F-15 practical.

Table 2.1 Physical Characteristics of the Airplanes (Ref. 7)

	Airplane					
	F-15	Lear 24	B-720	B-727	MD-11	PA-30
Typical mid-fuel weight, lb	35,000	11,000	140,000	160,000	359,000	3,000
Wing quarter chord sweep, deg	45	13	35	32	35	0
Wing span, ft	43	36	130	108	169.6	35.98
Wing area, ft <sup>2</sup>	608	231	2,433	1,700	3,958	178
Length, ft	64	43	137	153	192	25.16
Number of engines	2	2	4	3	3	2
Maximum thrust/engine, sea level static, lb	13,000*	2,900	12,500	15,000	60,000	(160 hp)

\*F-15 engine at intermediate power

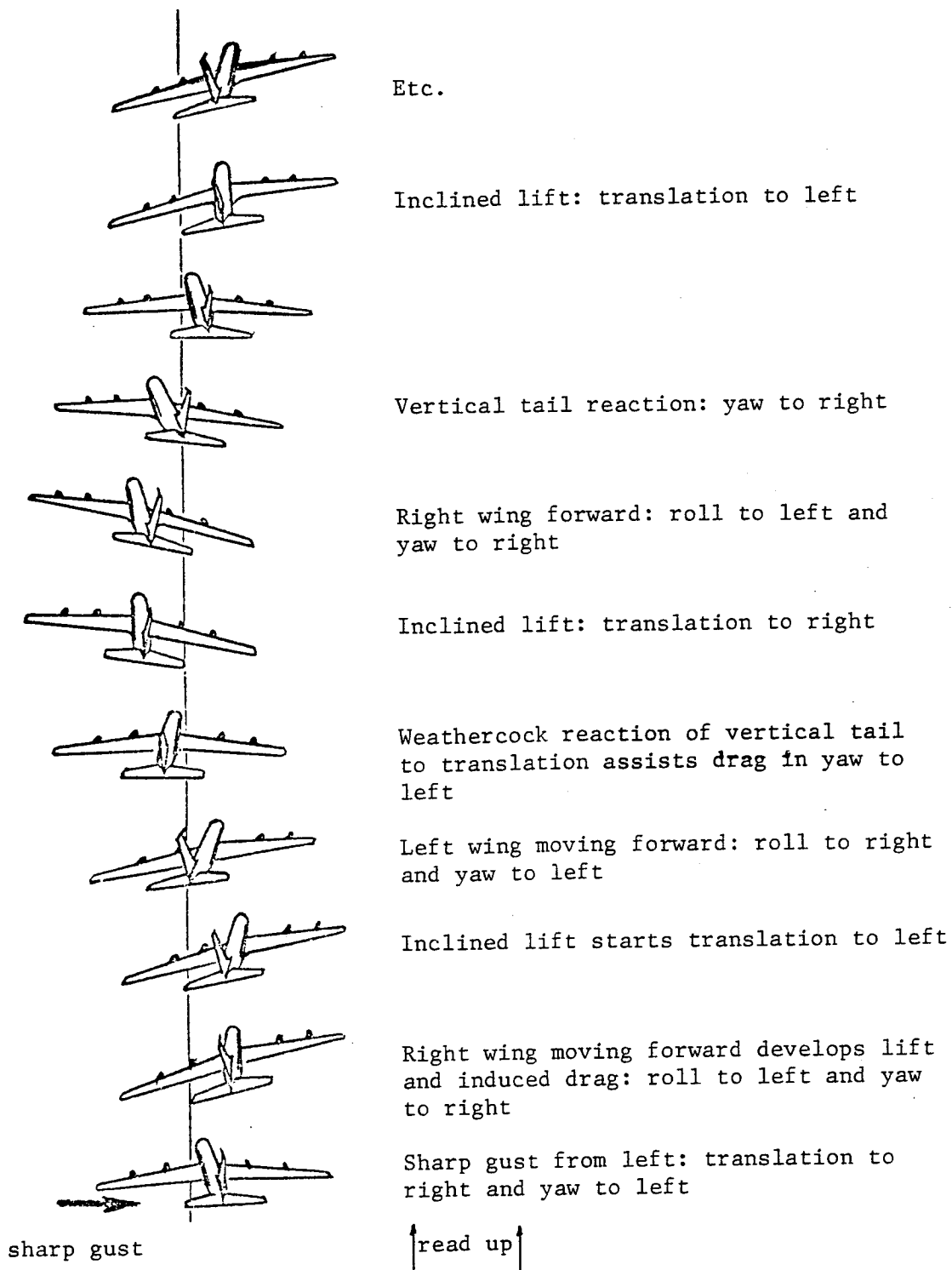


Figure 2.1 Dutch Roll Mode as Seen by an Outside Observer (Ref. 32)



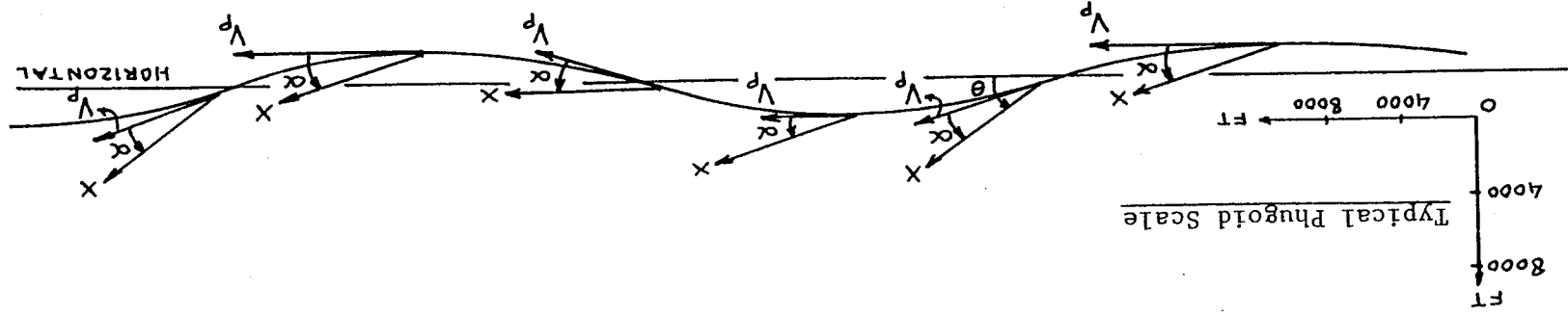


Figure 2.2 Phugoid Mode as Seen by an Outside Observer (Ref. 32)

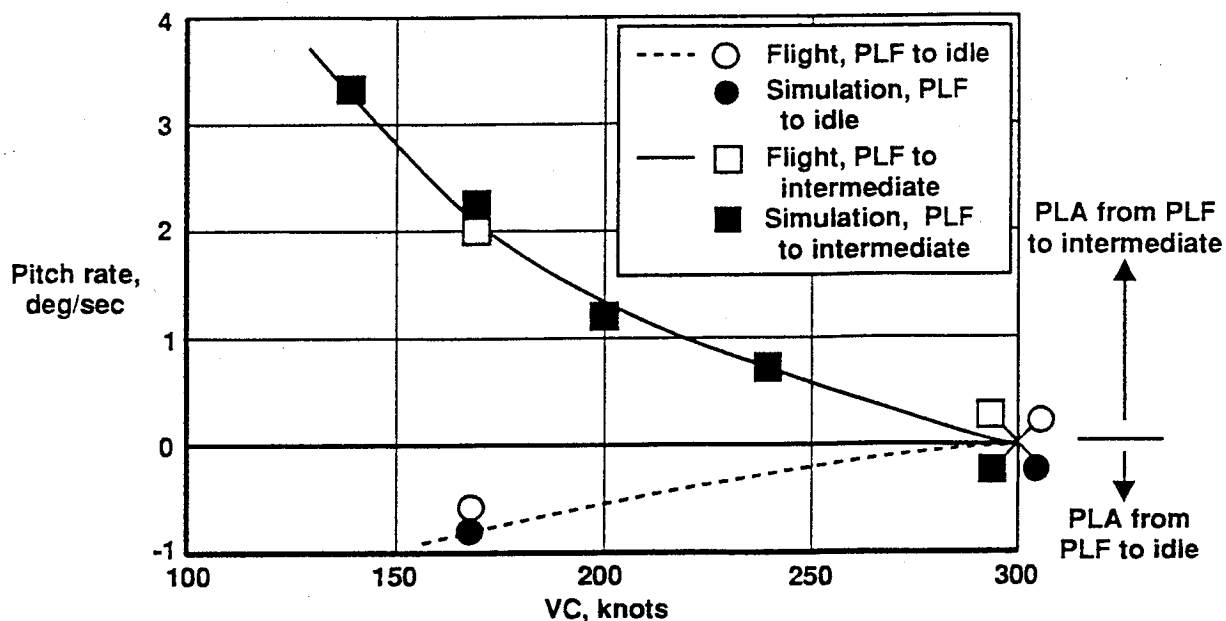


Figure 2.3 Effect of Speed on F-15 Flight and Simulation Maximum Pitch Rates (CAS Off) (Ref. 7)

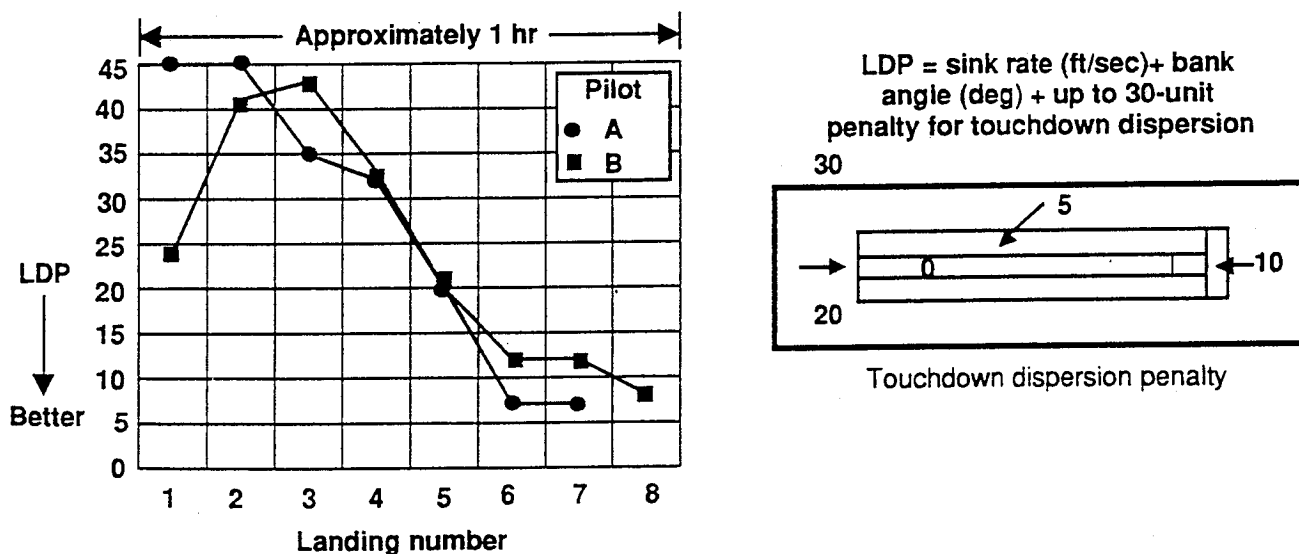


Figure 2.4 Landing Difficulty Parameter (LDP) for F-15 Simulation Flown with Manual Throttles-Only Control (Trim Airspeed 170 knots) (Ref. 7)

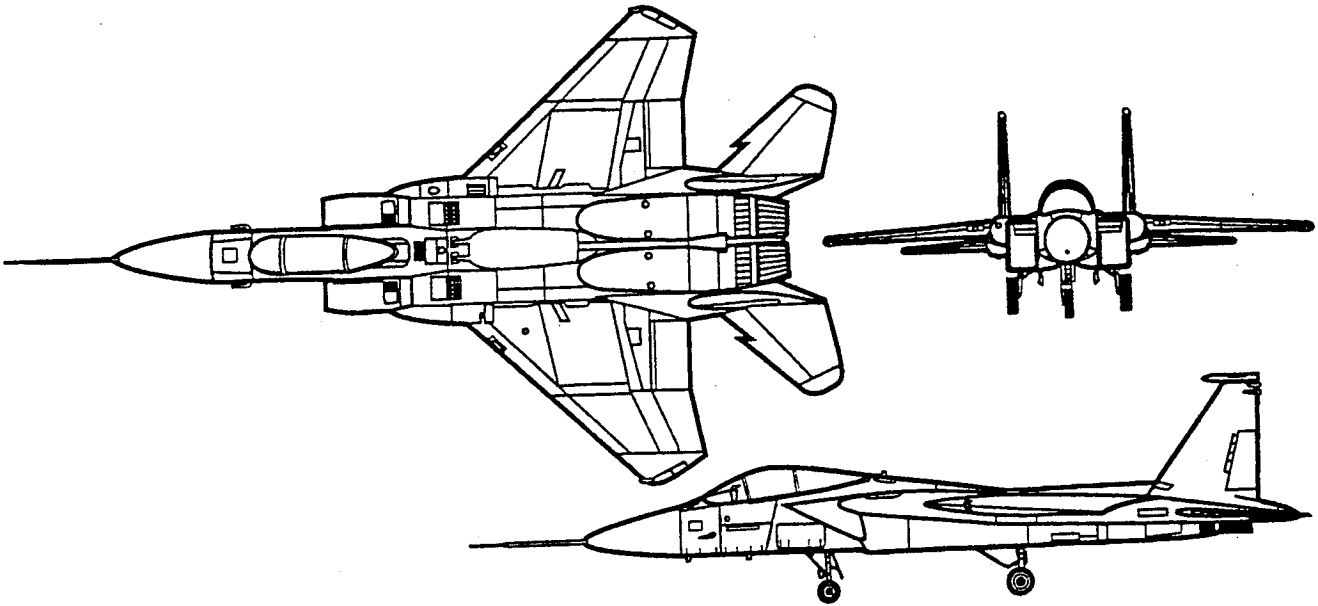


Figure 2.5 The F-15 Air Superiority Fighter (Ref. 7)

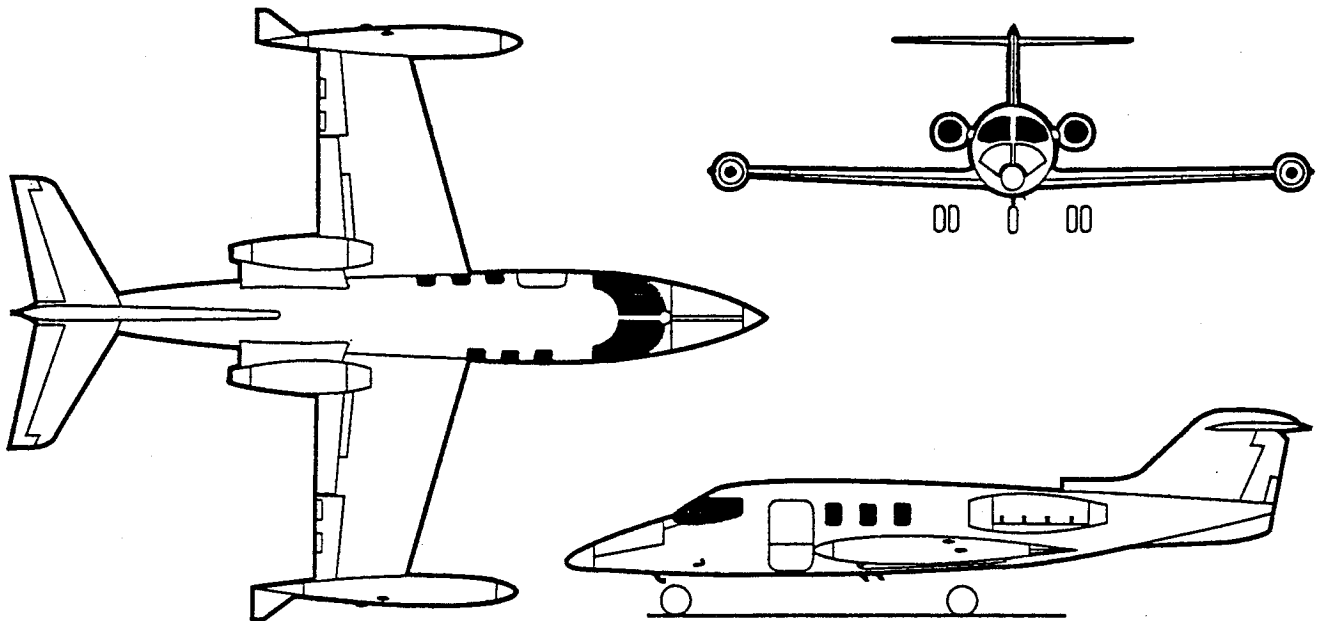


Figure 2.6 The Lear 24 Executive Jet (Ref. 7)

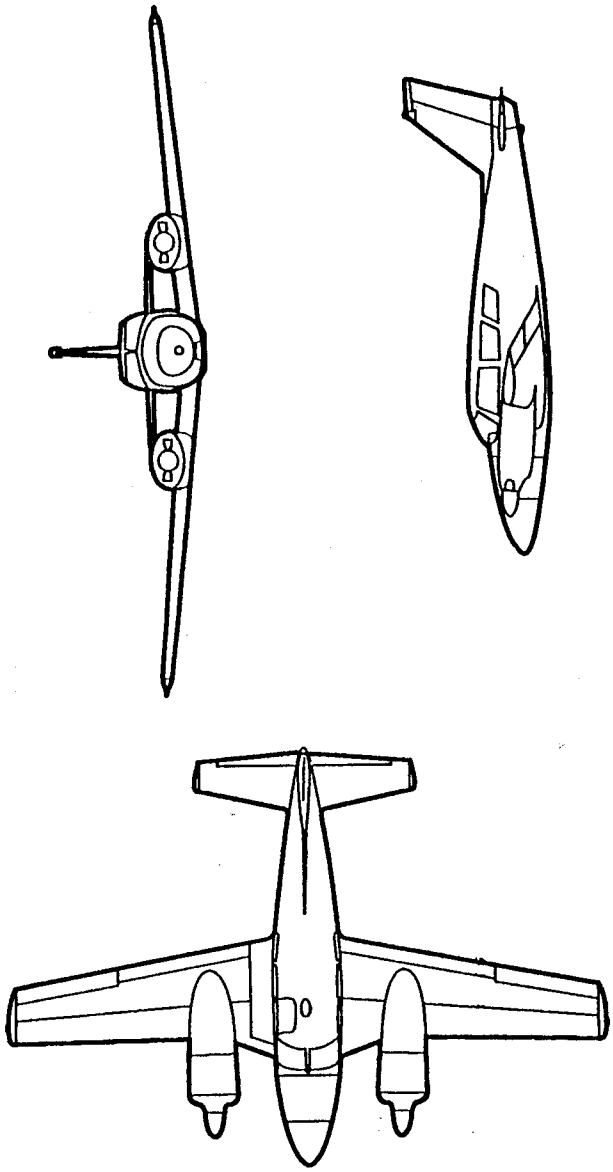


Figure 2.7 The PA-30 Light Twin-Engine Airplane (Ref. 7)

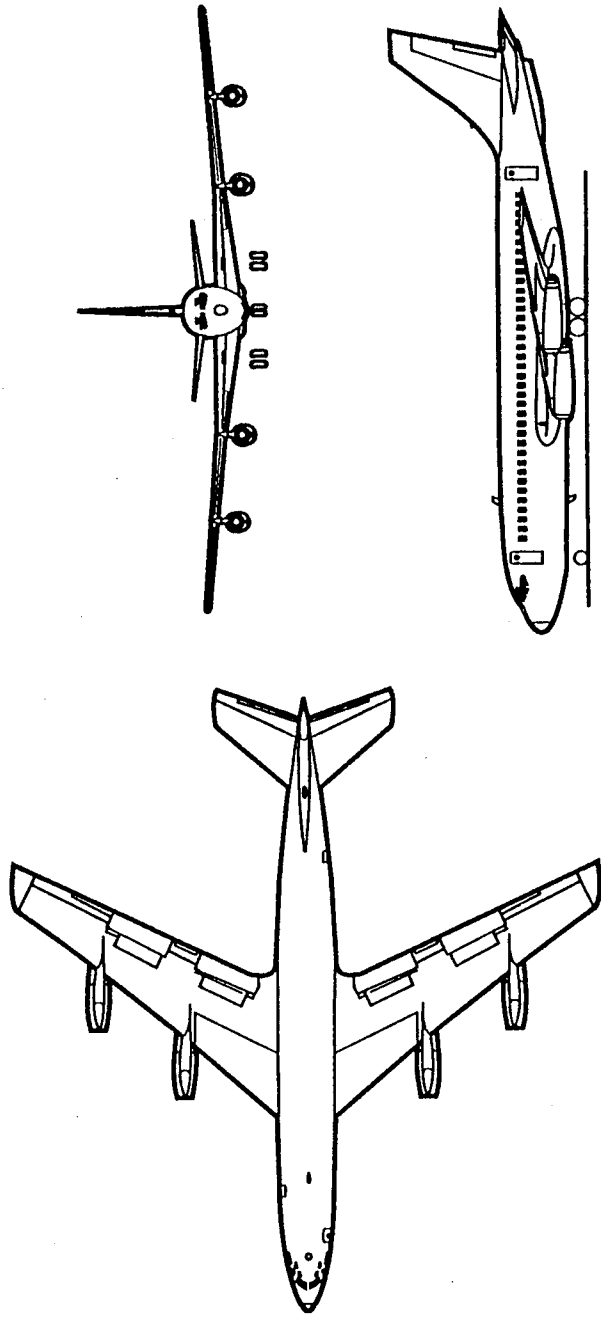


Figure 2.8 The B-720 Commercial Jet Transport (Ref. 7)

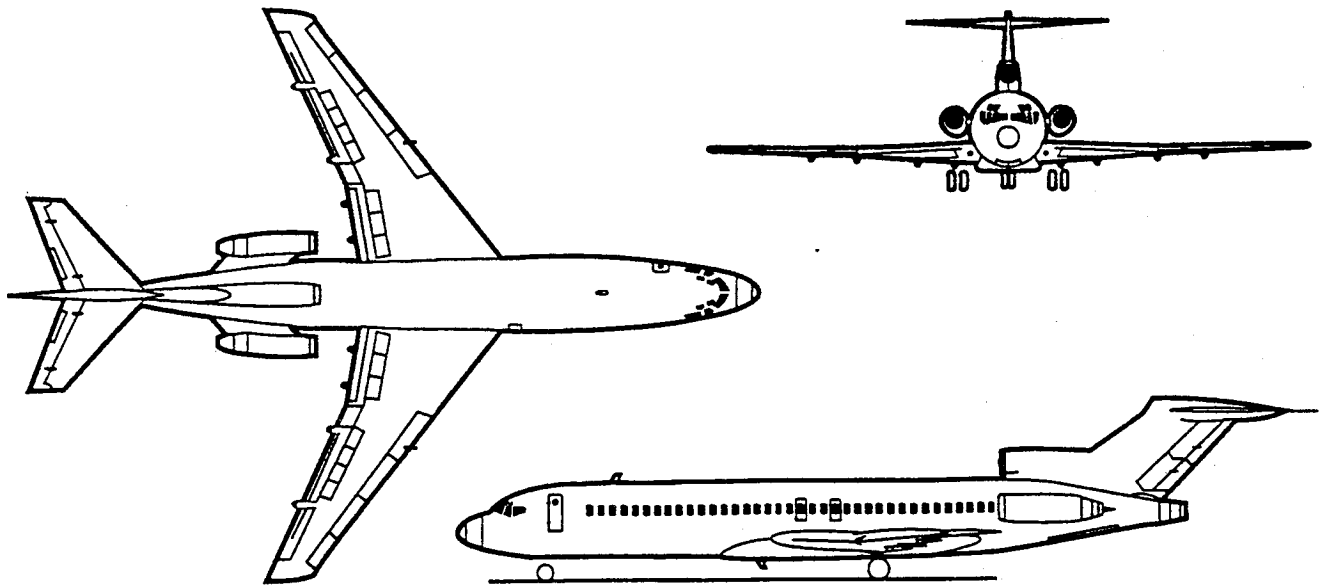


Figure 2.9 The B-727 Commercial Jet Transport (Ref. 7)

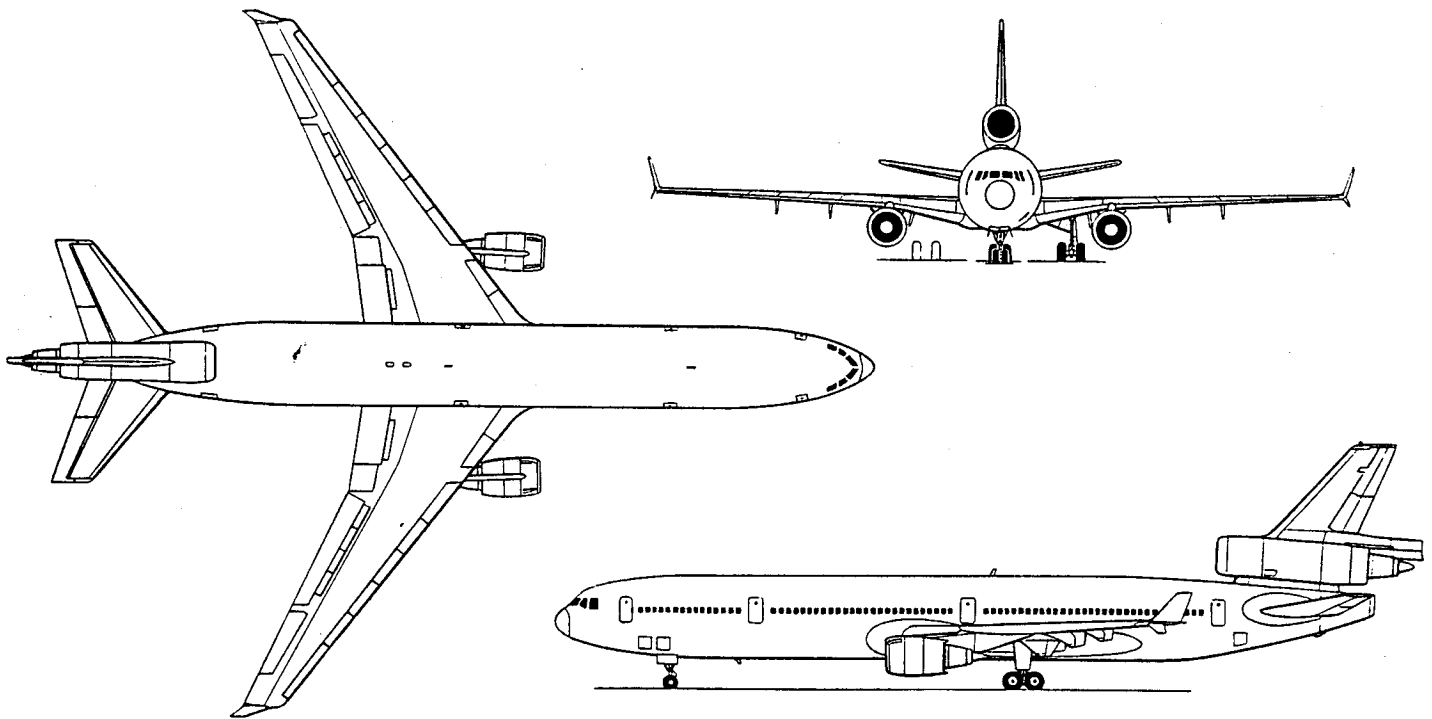


Figure 2.10 The MD-11 Commercial Jet Transport (Ref. 34)

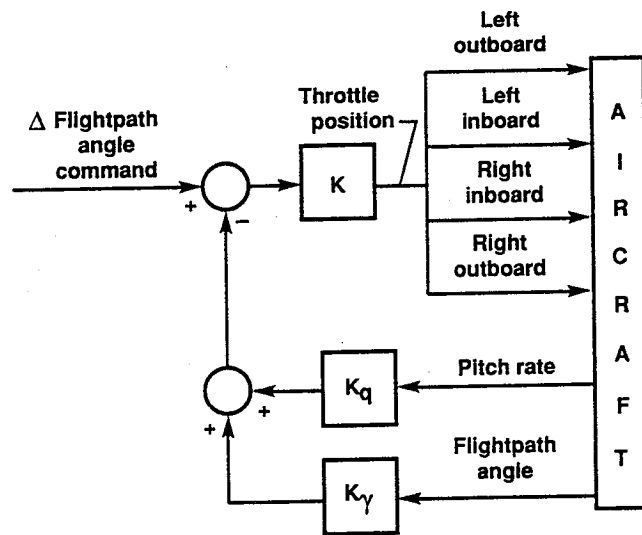


Figure 2.11 Longitudinal Block Diagram - Flight Path Angle Control (Ref. 9)

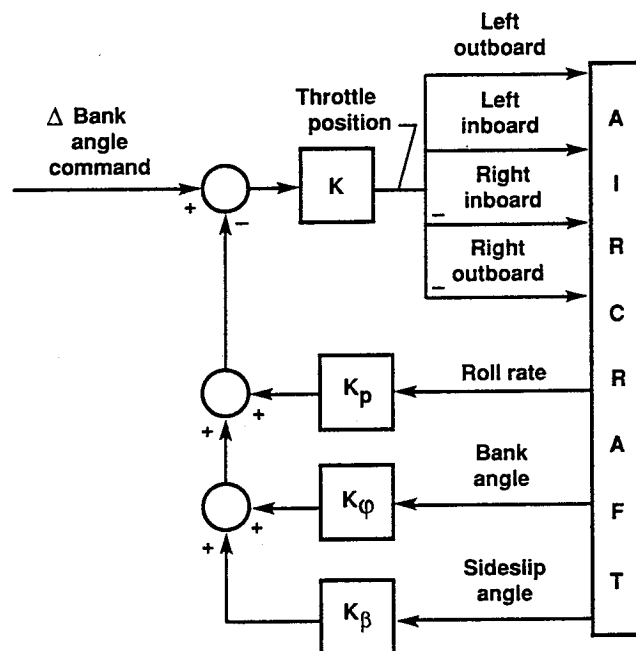


Figure 2.12 Lateral-Directional Block Diagram - Bank Angle and Heading Control (Ref. 9)

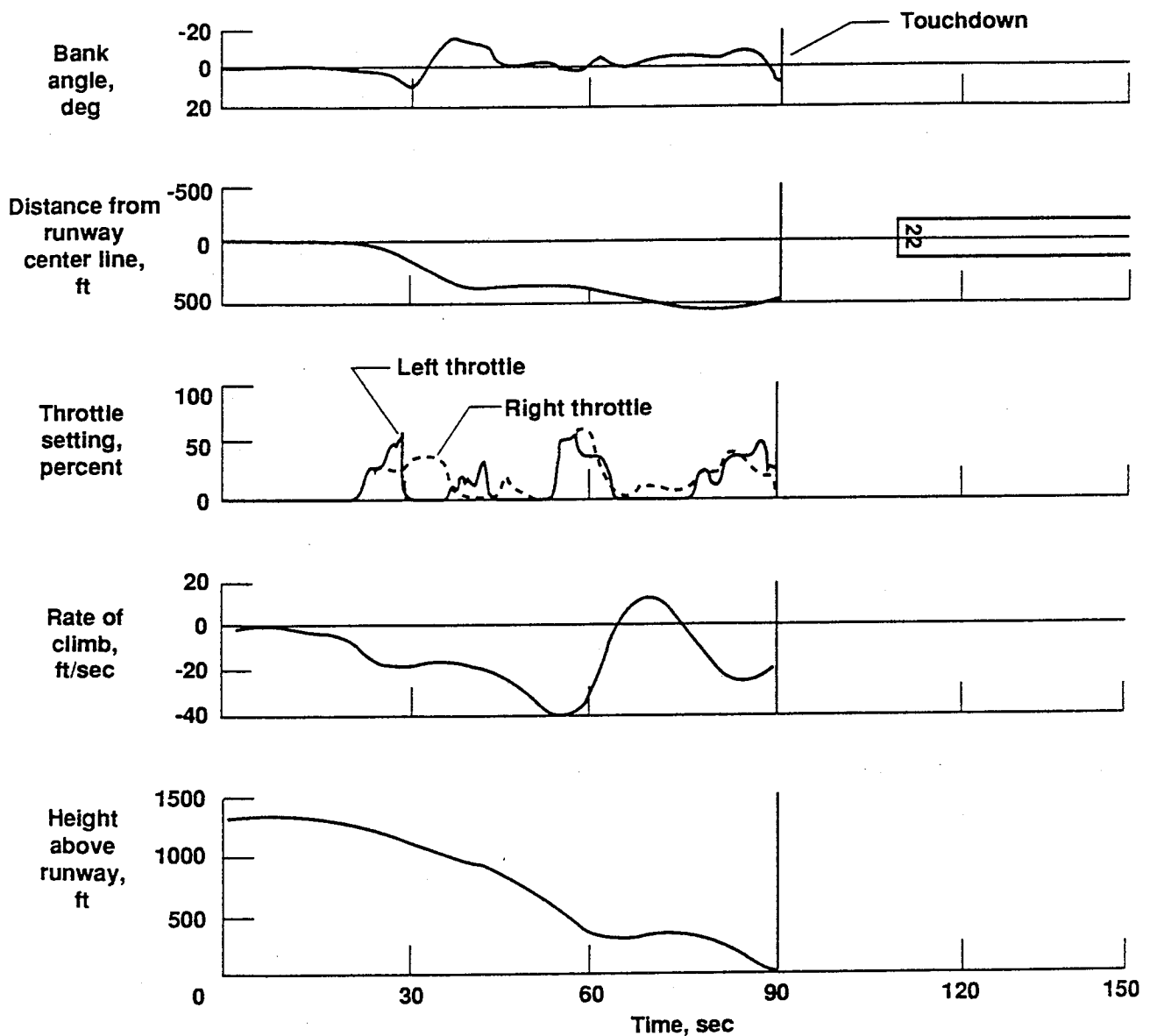


Figure 2.13 Time History of Throttles-Only Manual Landing of the F-15 Simulation (Trim Airspeed 170 knots - Pilot Inexperienced with Manual Throttles-Only Control)  
(Ref. 7)

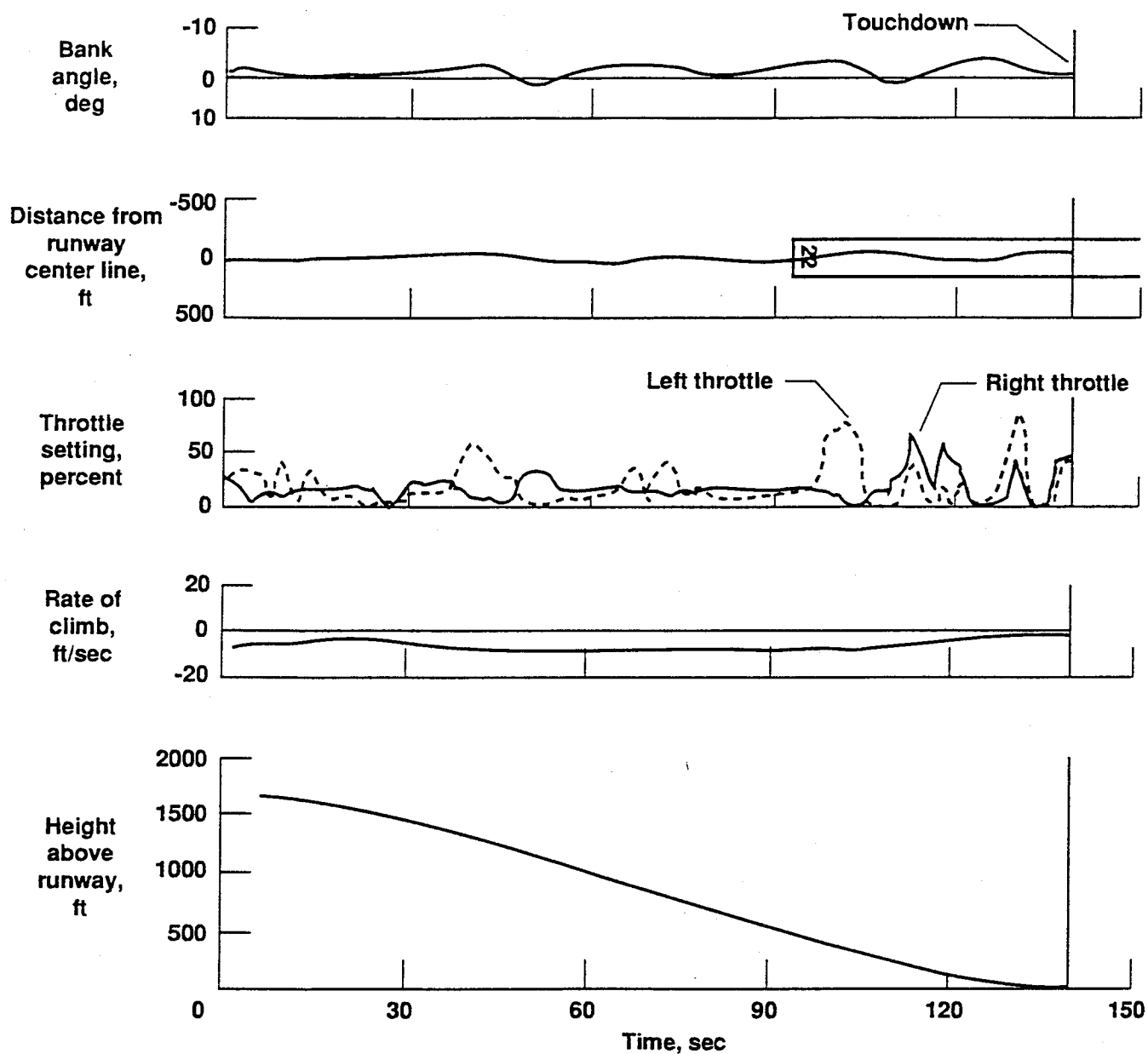


Figure 2.14 Time History of Augmented Throttles-Only Landing of  
the F-15 Simulation (Trim Airspeed 170 knots -  
Inexperienced Pilot's First Landing Using System)  
 (Ref. 7)



## CHAPTER 3

### OUTLINE OF PROPOSED WORK

#### 3.1. INTRODUCTION<sup>7,17,19,32,35,36,37</sup>

In the absence of control power due to primary control system failure, control power generated by selective application of engine thrust has proven to be a viable alternative. NASA Dryden has demonstrated the feasibility of controlling an aircraft during level flight, approach, and landing conditions using an augmented throttles-only control system. This system has been successfully flown in the flight test simulator for the B-720 passenger transport and the F-15 air superiority fighter and in actual flight tests for the F-15 aircraft.

The Douglas Aircraft Company is developing a similar system for the MD-11 aircraft. The simulator results show that the augmented throttles-only control system performance is promising. These results have been substantiated with actual flight data and additional flight tests are planned for the future. These aircraft may be controllable using engine thrust to supplement or replace the flight control system, but exactly how adequate are the flying qualities of the airplane when using engine thrust to control the flight path of the airplane?

All commercial transports must meet certain flying quality requirements before they are deemed certifiable. In the United States, commercial aircraft operating under ordinary flight conditions

are required to meet FAR 25 regulations. From an aircraft designer's viewpoint, these regulations can be considered to be met if the airplane meets Level 1 flying qualities as defined in the current USAF Military Specification - Flying Qualities of Piloted Airplanes document. The specifications are given in numerical tables and graphs, thereby establishing analytical criteria by which to measure whether or not the aircraft achieves the desired handling qualities.

In specifying handling quality criteria, it is necessary to recognize differences in types of aircraft, in types of flying maneuvers to be performed during some phase of flight, and in failure states of airplane systems. These differences are recognized in the flying qualities specifications and are defined in Tables 3.1 - 3.4.

The flying quality levels as defined in Table 3.3 are tied in with the Cooper-Harper pilot rating scale. This scale represents a very successful attempt to relate pilot comments about the ease or difficulty with which airplanes can be controlled in certain flight situations to a numerical rating. The Cooper-Harper scale is shown in Table 3.5. The tie-in with the flying quality levels as previously defined is indicated in the table.

In view of the current development and promising test results of the throttles-only control system, it seems reasonable to ask the following questions:

- Is it possible to arrange the engines in a large passenger transport in such a way that flight path control using only the augmented throttles-only control system is not only possible, but meets Level 1 or Level 2 handling quality requirements?

- Since total failure of the primary flight control system can be caused by the failure of an engine, can the number of engines and their arrangement be selected such that flight path control with one engine inoperative is still possible with Level 1 or Level 2 handling quality requirements?

- Can one or more levels of primary flight control system redundancy be eliminated in an airplane equipped with a Level 1 or Level 2 augmented throttles-only control system, allowing the engine thrust to be used as a backup flight control system?

- What are the weight, drag, systems design, and cost benefits associated with such a design?

The proposed research work which addresses these issues will be carried out in phases which will be described in the following sections.

### 3.2. FAMILIARIZATION WITH PREVIOUS NASA WORK AND APPLICABLE NASA RESEARCH TOOLS<sup>9,19,38</sup>

Previous NASA work in this area was discussed in Chapter 2. Applicable NASA research tools include a batch simulation which can be run on a SUN SPARC workstation as well as a real-time simulation.

A six-degree-of-freedom, real-time simulation of the B-720 aircraft was developed by interfacing the models for the aerodynamics, control systems, actuators, gear dynamics, and engines of the aircraft to a fixed-base cockpit with user interfaces. The B-720 model was selected because a high-fidelity fixed-base simulation

of the aircraft was available based on an earlier NASA/FAA controlled impact flight test program in 1984 to further the technology for improving crash survivability onboard a transport aircraft. Because only limited envelope models were needed, the existing simulation primarily reflects the low-speed/low-altitude flight conditions required for the impact demonstration.

The B-720 simulation is currently interfaced with a fixed-base cockpit of a modified F-15 fighter. The F-15 has only two throttle levers, therefore the inboard and outboard engines on each wing of the B-720 are grouped together. This grouping has not been considered a serious limitation for throttles-only control studies thus far.

The cockpit provides the basic instruments necessary to operate the B-720 aircraft. A photograph of the cockpit layout appears in Figure 3.1. In addition to flight instrumentation, the pilot has fingertip control of the simulation through a series of switches that enables him to hold, reset, or operate the simulation, initiate strip chart recording, vary or capture initial conditions, or select automatic trim features. A field of general purpose toggle switches is also provided at the cockpit and is currently used to initiate a control surface failure, initiate an engine failure, enter a propulsion-only control mode, or activate an automatic landing system.

A flight control system failure is simulated by bypassing the actuator model at the activation of a switch, thus locking the surfaces at their last position. In addition to the throttles, the pilot still has control of the flaps and the stabilizer which are electrically controlled. Separate switches are used to activate the engines-only

augmented control modes in the longitudinal and lateral directions for independent study.

The simulation has dynamic 'out the window' runway scenes displaying a 160 square nautical mile area of Edwards Air Force Base with its various runways on a 19 inch graphics display unit.

The B-720 simulation also includes a continuous random turbulence model that calculates turbulence velocities and angular rates ( $u$ ,  $v$ ,  $w$ ,  $p$ ,  $q$ , and  $r$ ). Crosswind components can also be added as a function of altitude.

The aerodynamic model for the B-720 aircraft is implemented based on the manufacturer's documents. The data from both wind tunnel and flight tests were reduced to support only the low altitude and Mach flight envelope.

Each aerodynamic coefficient is the sum of individual aerodynamic terms made up of nondimensional derivatives and coefficient deltas. These terms are obtained by table lookup and linear interpolation. Ground effects and the effects of c.g. position change are also modeled.

The B-720 aircraft uses the JT3C-7 turbojet engine. The simulation uses a modified J-57 turbojet engine simulation model that includes control servo dynamics. The model has both table lookup functions and dynamic elements.

The batch simulation uses the same turbulence, aerodynamic, and engine models as the real-time simulation. The input commands, whether an input function to the batch simulation or a control stick input to the real-time simulation, as well as the calculated output parameters, are plotted in graphical form. Figure 3.2 shows plots of

the input commands and the output parameters for a B-720 approach and landing using the real-time simulation.

### 3.3. BASELINE DESIGN OF A MEGA-TRANSPORT<sup>17,39,40,41</sup>

An ultra-high capacity aircraft, or mega-transport, will be designed utilizing the Advanced Aircraft Analysis (AAA) design program. AAA is an interactive computer program which was developed by Design, Analysis and Research Corporation in conjunction with the University of Kansas to perform preliminary design and analysis functions for fixed wing aircraft.

The mission specifications and mission profile are presented in the following subsections.

#### 3.3.1. Mission Specifications

- Role
  - 800 passenger capacity commercial jet transport aircraft
- Crew
  - 2 flight crews - each flight crew consisting of 1 pilot and 1 co-pilot
  - 16 flight attendants
- Payload
  - Each crewmember is allowed 30 lb of baggage
  - Each passenger is allowed 40 lb of baggage

- Performance
  - Range : 5,000 nautical miles
  - Cruise Speed : M = 0.85 at 35,000 ft
  - Cruise Altitude : 35,000 ft
  - Service Ceiling : 40,000 ft
  - Field Length : 10,000 ft @ 5,000 ft field elevation, 95° F day
  - Climb : Direct climb to cruise altitude
- Powerplant
  - 4 - 6 turbofan engines
- Certification
  - FAR 25
- Fuel Reserves
  - Must meet FAR 121.645 fuel supply requirements for turbine-engine-powered flag carrier operations.

### 3.3.2. Mission Profile

FAR 121.645 states, in part, that no turbine-engine-powered flag carrier may be dispatched unless it has enough fuel:

- to fly and land at the airport to which it is released;
- after that, to fly for a period of 10 percent of the total time required to fly from the airport of departure to, and land at the airport to which it was released;
- after that, to fly to and land at the most distant alternate airport specified in the flight release, if an alternate is required; and

- after that, to fly for 30 minutes at holding speed at 1,500 feet above the alternate airport under standard temperature conditions.

The conditions of the FAR 121.645 fuel requirements determine the mission profile of the mega-transport as follows. The mission profile consists of the following 14 mission segments:

- Warmup
- Taxi
- Takeoff to destination airport
- Climb to cruise altitude
- Cruise to destination airport
- Loiter for a time period equal to 10 percent of the total time required to fly from the airport of departure to, and land at the airport to which it was released
- Descent
- Land/Taxi
- Takeoff to alternate airport
- Climb to intermediate altitude
- Cruise to alternate airport
- Loiter for a time period of 30 minutes at holding speed at 1,500 feet above the alternate airport
- Descent
- Land/Taxi.

The mission profile of the mega-transport is shown in Figure 3.3.



### 3.3.3. Summary of the Mega-Transport Data<sup>40</sup>

A preliminary three-view of the mega-transport is shown in Figure 3.4. A summary of the geometry, weight, drag polar, and performance sizing data which have been calculated thus far for the mega-transport is presented in Table 3.6. Table 3.7 contains the nondimensional stability and control derivatives for the mega-transport.

The longitudinal transfer functions, flying quality parameters, and flying quality levels for both cruise and approach conditions are found in Tables 3.8 - 3.11. Figures 3.5 and 3.6 show the short-period frequency requirements for the cruise and approach conditions. The lateral-directional transfer functions, flying quality parameters, and flying quality levels for both cruise and approach conditions are found in Tables 3.12 - 3.17. Figures 3.7 and 3.8 show the minimum dutch roll frequency and damping ratio requirements for the cruise and approach conditions.

### 3.4. DEVELOP A SIMULATION OF THE MEGA-TRANSPORT<sup>17,34,40</sup>

A simulation of the mega-transport will be developed for the batch simulation as well as for the real-time simulator. The aerodynamic data will be developed by using the parameters which were calculated in the design phase of the mega-transport (which includes the data in Tables 3.6 - 3.17 along with the external dimensions of the aircraft and the c.g. envelope). These data, along

with flight condition information, will be used to modify the existing B-720 aerodynamic data decks.

The JT3C-7 turbojet engine data will be replaced with a Pratt and Whitney PW 4084 turbofan engine deck. The PW 4084 turbofan is scheduled to be installed on the new Boeing 777 passenger transport and is much more representative of the high thrust/fuel efficient turbofan engines currently available to power the next generation of passenger transports than the older JT3C-7 turbojet engine.

### 3.5. MEGA-TRANSPORT SIMULATION FLYING QUALITIES EVALUATION<sup>17,32</sup>

Several parameters which could affect the flying qualities of the mega-transport will be varied on the mega-transport simulation and flown, both with and without the augmented throttles-only flight control system engaged. Some of the parameters which will be examined are:

- number of engines
- placement of engines [vertical and lateral]
- engine out
- engine time constants
- flaps/slats/gear
- center of gravity.

The simulator will be flown in both cruise and approach-to-land flight conditions. The flying qualities of the mega-transport in a

particular configuration will be evaluated by having the flight test pilot fly a specified task and then assign the flying qualities a rating number on the Cooper-Harper scale. The objective is to determine under what conditions Level 1 or Level 2 flying qualities are obtainable during cruise and approach flight phases with total primary flight control system failure using either manual thrust input or augmented throttles-only flight control system input to control the flight path.

### 3.6. MEGA-TRANSPORT SIMULATION FLYING QUALITIES ANALYSIS<sup>17,32,42,43,44,45,46,47,48,49</sup>

Although the Cooper-Harper rating is a very successful method used to evaluate the handling qualities of an airplane under certain flight conditions, the evaluation is subject to the pilot's opinion of the ease or difficulty of flying the assigned task. Pilot opinions are likely to vary depending on factors such as pilot training, knowledge, experience, physical condition, and ability to assess the specific task.

Because of the subjective nature of evaluating flying qualities based solely on pilot opinion, it is desirable to quantify these Cooper-Harper rating results by analytically examining the performance of the human pilot/engine/airframe combination from the viewpoint of the closed loop system shown in Figure 3.9. To perform closed loop analysis on the pilot/engine/airframe system, it is necessary to have available a mathematical model of the basic aircraft characteristics, the engine time constants, and the human pilot.

The basic aircraft response to a specified input is characterized by the longitudinal and lateral-directional airplane transfer functions, which depend on the dimensional stability derivatives. These stability derivatives take into account factors such as the weight, geometry, inertia, and flight condition of the airplane. The effects of varying the number of engines, placement of engines, engine out condition, flaps/slats/gear configuration, and center of gravity location can be examined through the effects these parameters have on the weight, geometry, and inertia of the airplane.

The number of engines, placement of engines, engine out condition, flaps/slats/gear configuration, and center of gravity location will all affect the geometry and/or inertia of the airplane. In addition, the number of engines will affect the airplane weight in the following two ways:

- additional engines means additional weight
- number and placement of engines affect wing weight.

The wing weight is a function of many factors such as shear forces, bending moments, stress levels, and material properties. These, in turn, depend upon the number and placement of engines. Torenbeek (Ref. 48) has developed a design-sensitive weight prediction method for wing structures which can be used to modify the wing weight according to the number of engines and their location on the wing.

Varying the number and location of engines, engine out condition, flaps/slats/gear configuration, and center of gravity parameters affect the stability derivatives and, hence, the transfer

functions of the airplane. The response (transfer function) of most interest to the pilot using engine thrust alone to maneuver the airplane is how the flight path angle and bank angle of the airplane respond to change in throttle control, the desired transfer functions being  $(\gamma/\delta T)$  and  $(\phi/\delta T)$ , respectively.

The engine time constant, the time it takes the engine to produce the commanded thrust, is primarily a function of the spool up time from the current thrust level to the commanded thrust level. The spool up time depends on many factors such as gas temperature, pressure levels, engine materials, radial and axial clearances, variable stator vane position, rotor balance, aerodynamic matching of components, inlet flow conditions, and age of the engine. The engine time constant can be modeled by a simple first-order lag,  $(1/(T_{\text{engs}} + 1))$ .

The primary objective of most of the past experimental and analytical programs to develop mathematical descriptions for pilot response characteristics has been to achieve reasonable descriptions of the pilot as a component in the engineering system. Major efforts in model building have thus been placed on the evolution of models which can predict pilot dynamic response characteristics of engineering significance, but which are otherwise of minimum analytical complexity. Such models are conceptual descriptions of the human. There are a number of possible models with increasing complexity and an increasing number of parameters. All have special merits in that they can describe or model certain general or more specific measured characteristics of human control behavior.

The choice of model is dependent upon the choice of task to be analyzed. Most of the laboratory tasks applied in human control research fall into either disturbance tasks (approach for landing while the airplane is perturbed by atmospheric turbulence) or target tasks (wing man flying formation with lead airplane). For the case of trying to control and land an airplane using throttles alone, the disturbance model is selected to be most representative of the pilot's task.

Van der Vaart (Ref. 49) has developed a simple linear human pilot model fitted to measured frequency response data for a disturbance task. The model is given in Equation 3.1:

$$H_p(\omega) = K_p \frac{\tau_{den} [1 + j\omega\tau_{num}]}{\tau_{num} [1 + j\omega\tau_{den}]} [1 + j\omega\tau_L] e^{-j\omega\tau_e} \quad [\text{Eqn. 3.1}]$$

where:

$H_p(\omega)$	human pilot transfer function
$K_p$	gain constant of the pilot ( $K_p = 1.04$ )
$\tau_{den}$	denominator (lag) time constant in low-frequency extension of pilot model ( $\tau_{den} = 4.09$ sec)
$\tau_e$	equivalent time delay ( $\tau_e = 0.25$ sec)
$\tau_L$	lead time constant of the pilot ( $\tau_L = 0.65$ sec)
$\tau_{num}$	numerator (lead) time constant in low-frequency extension of pilot model ( $\tau_{num} = 2.21$ sec).

Figure 3.10 shows the measured pilot response along with the fitted pilot model for a disturbance task. The pilot model fits the measured data extremely well except for a slight peak in the high frequency range. Considering the frequency at which the peak occurs (around 10 radians/second), it might well be due to the neuro-muscular system. Such a peak can be modeled by the frequency response function given in Equation 3.2:

$$H_N(\omega) = \frac{1}{[1 + (2\zeta j\omega/\omega_0) + (j\omega/\omega_0)^2]} \quad [\text{Eqn. 3.2}]$$

where:

$H_N(\omega)$	frequency response of neuro-muscular dynamics
$\zeta$	damping ratio
$\omega_0$	undamped natural frequency.

Typical values for the damping ratio and the undamped natural frequency are  $\zeta = 0.15$  and  $\omega_0 = 16.5$  radians/second, respectively. Van der Vaart found that by extending the pilot model given in Equation 3.1 with a model for the neuro-muscular dynamics and by using similar parameter values, a better fit of the high frequency peaks can be obtained. However, when calculating the error root-mean-square based on a model with neuro-muscular dynamics, it turned out that only negligible differences are found relative to the case for the model without neuro-muscular dynamics. Therefore, the neuro-muscular dynamics are ignored.

Bode and root-locus analyses are two methods used to study the stability behavior of closed loop systems such as that shown in Figure 3.9. These methods will be used to analyze the behavior of the pilot/engine/mega-transport system in a particular configuration, explain the reasons behind a Cooper-Harper rating, by examining what influence the parameters under investigation have on the system dynamics and, hence, flying qualities of the airplane, and determine the 'design drivers' which most influence the flight path control response of the airplane using engine thrust alone.

### 3.7. DETERMINATION OF BENEFITS ASSOCIATED WITH AUGMENTED THROTTLES-ONLY CONTROL SYSTEM<sup>17</sup>

Designing an aircraft such that Level 1 or Level 2 flying qualities are obtained using the augmented throttles-only control system should insure that one level of redundancy can be reduced in the flight control system. An augmented throttles-only flight control back-up system could enable the aircraft manufacturers to reduce the number of hydraulic systems in the aircraft (or reduce or eliminate mechanical cable backup for fly-by-wire control systems).

A trade study should be performed comparing the weight and the cost associated with the purchase, installation, and maintenance of both the augmented throttles-only control system and the conventional redundant hydraulic back-up system. This study would indicate which system was economically more feasible. Aircraft manufacturers, while concerned with the relative costs of these



systems, should not lose sight of the primary benefit of the augmented throttles-only control system - saving human lives. The level of passenger and flight crew safety could be improved as the complete loss of the flight control system would no longer render an aircraft uncontrollable.

Table 3.1 Classification of Airplanes (Ref. 37)

- Class I  
Small, light airplanes such as:
  - Light utility
  - Primary trainer
  - Light observation
  
- Class II  
Medium weight, low-to-medium maneuverability airplanes such as:
  - Heavy utility/search and rescue
  - Light or medium transport/cargo/tanker
  - Early warning/electronic countermeasures/airborne command, control, or communications relay
  - Antisubmarine
  - Assault transport
  - Reconnaissance
  - Tactical bomber
  - Heavy attack
  - Trainer for Class II
  
- Class III  
Large, heavy, low-to-medium maneuverability airplanes such as:
  - Heavy transport/cargo/tanker
  - Heavy bomber
  - Patrol/early warning/electronic countermeasures/airborne command, control, or communications relay
  - Trainer for Class III
  
- Class IV  
High maneuverability airplanes such as:
  - Fighter/interceptor
  - Attack
  - Tactical reconnaissance
  - Observation
  - Trainer for Class IV

Table 3.2 Flight Phase Categories (Ref. 37)

Nonterminal Flight Phases

- Category A

Those nonterminal flight phases that require rapid maneuvering, precision tracking, or precise flight path control. Included in this Category are:

- a) Air-to-air combat (CO)
- b) Ground Attack (GA)
- c) Weapon delivery/launch (WD)
- d) Aerial recovery (AR)
- e) Reconnaissance (RC)
- f) In-flight refueling (receiver) (RR)
- g) Terrain following (TF)
- h) Antisubmarine search (AS)
- i) Close formation flying (FF)

- Category B

Those nonterminal flight phases that are normally accomplished using gradual maneuvers and without precision tracking, although accurate flight path control may be required. Included in this Category are:

- a) Climb (CL)
- b) Cruise (CR)
- c) Loiter (LO)
- d) In-flight refueling (tanker) (RT)
- e) Descent (D)
- f) Emergency descent (ED)
- g) Emergency deceleration (DE)
- h) Aerial delivery (AD)

Table 3.2 Flight Phase Categories (con't) (Ref. 37)

Terminal Flight Phases

- Category C

Terminal flight phases are normally accomplished using gradual maneuvers and usually require accurate flight path control. Included in this Category are:

- a) Takeoff (TO)
- b) Catapult takeoff (CT)
- c) Approach (PA)
- d) Wave-off/go-around (WO)
- e) Landing (L)

Table 3.3 Levels of Flying Qualities (Ref. 37)

- Level 1  
Flying qualities clearly adequate for the mission flight phase.
- Level 2  
Flying qualities adequate to accomplish the mission flight phase, but some increase in pilot workload or degradation in mission effectiveness, or both, exists.
- Level 3  
Flying qualities such that the airplane can be controlled safely, but pilot workload is excessive or mission effectiveness is inadequate, or both. Category A flight phases can be terminated safely, and Category B and C flight phases can be completed.

Table 3.4 Allowable Probability of Certain System Failures (Ref. 32)

- At Least Level 1 - for airplane normal (no failure) state
- At Least Level 2 - after failures that occur less than once per 100 flights
- At Least Level 3 - after failures that occur less than once per 10,000 flights

Flying quality levels below Level 3 are not allowed except under special circumstances.

Table 3.5 Cooper-Harper Pilot Opinion Rating Scale (Ref. 32)

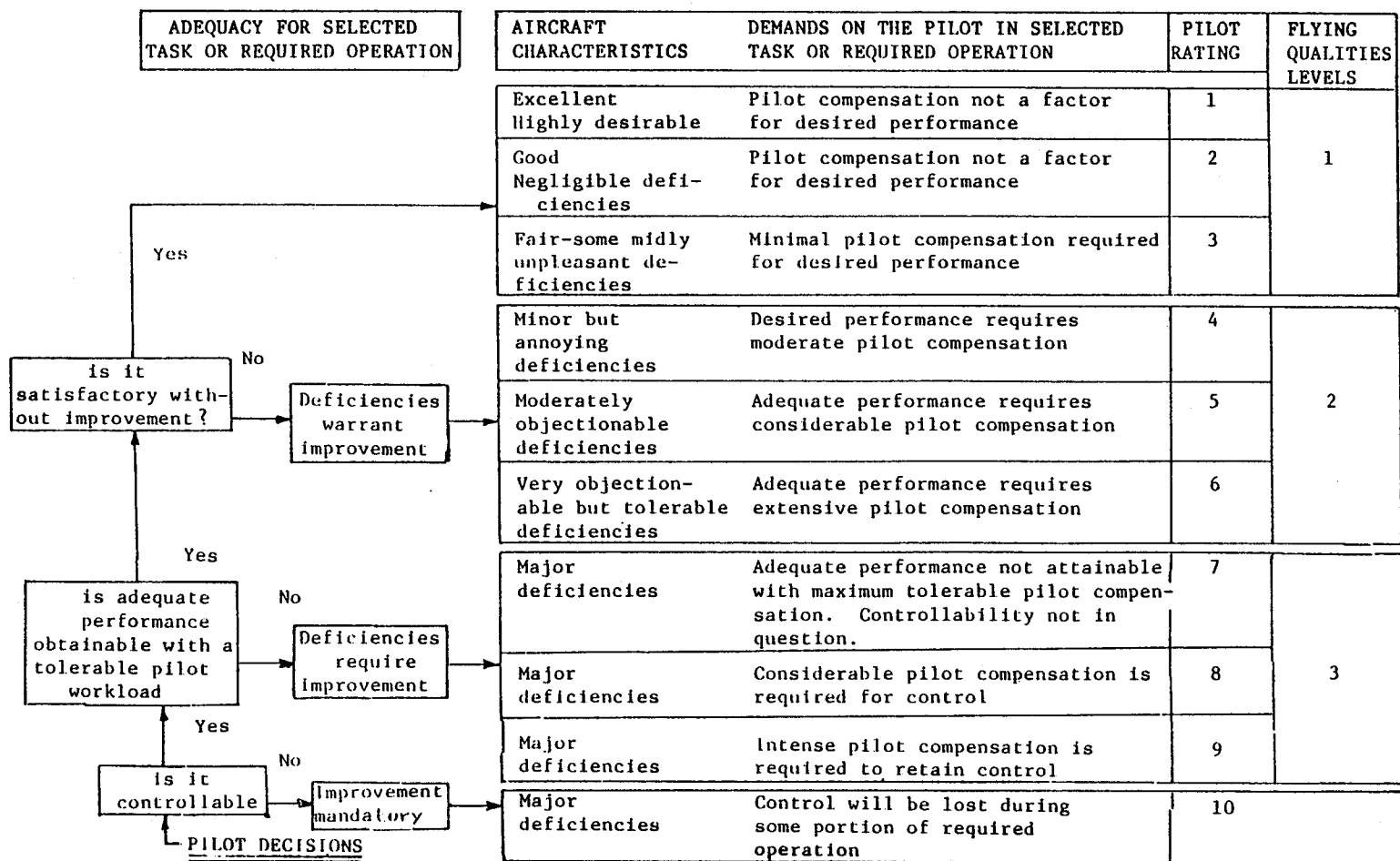


Table 3.6 Summary of the Geometry, Weight, Drag Polar, and  
Performance Sizing Data for the Mega-Transport

(Ref. 40)

GEOMETRY

Wing

- $S_w$ , wing area.....11,900 ft<sup>2</sup>
- $b_w$ , wing span.....318.0 ft
- $AR_w$ , wing aspect ratio.....8.5
- $\lambda_w$ , wing taper ratio.....0.30
- $\Lambda_{wc}/4$ , wing quarter-chord sweep.....30 deg
- $C_w$ , wing mean geometric chord.....41.0 ft
- $C_{rw}$ , wing root chord.....57.6 ft
- $C_{tw}$ , wing tip chord.....17.3 ft

Horizontal Tail

- $S_h$ , horizontal tail area.....2,800 ft<sup>2</sup>
- $b_h$ , horizontal tail span.....105.8 ft
- $AR_h$ , horizontal tail aspect ratio.....4.0
- $\lambda_h$ , horizontal tail taper ratio.....0.34
- $\Lambda_{hc}/4$ , horizontal tail quarter-chord sweep.....35 deg
- $C_h$ , horizontal tail mean geometric chord.....28.6 ft
- $C_{rh}$ , horizontal tail root chord.....39.5 ft
- $C_{th}$ , horizontal tail tip chord.....13.4 ft

Vertical Tail

- $S_v$ , vertical tail area.....2,051 ft<sup>2</sup>
- $b_v$ , vertical tail span.....57.3 ft
- $AR_v$ , vertical tail aspect ratio.....1.6
- $\lambda_v$ , vertical tail taper ratio.....0.35
- $\Lambda_{vc}/4$ , vertical tail quarter-chord sweep.....37 deg
- $C_v$ , vertical tail mean geometric chord.....38.6 ft
- $C_{rv}$ , vertical tail root chord.....53.0 ft
- $C_{tv}$ , vertical tail tip chord.....18.6 ft

Table 3.6 Summary of the Geometry, Weight, Drag Polar, and  
Performance Sizing Data for the Mega-Transport  
 (con't) (Ref. 40)

GEOMETRY (con't)

Fuselage

- L<sub>fus</sub>, fuselage length.....277 ft
- D<sub>fus</sub>, average fuselage diameter.....25 ft

WEIGHT

- W<sub>PL</sub>, payload weight.....185,900 lb
- W<sub>crew</sub>, crew weight.....4,100 lb
- W<sub>E</sub>, empty weight.....683,400 lb
- W<sub>F</sub>, fuel weight.....541,400 lb
- W<sub>tfo</sub>, trapped fuel and oil weight.....7,110 lb
- W<sub>TO</sub>, gross takeoff weight.....1,421,900 lb

DRAG POLARS

- |                      |                               |
|----------------------|-------------------------------|
| • Takeoff, gear down | $C_D = 0.0464 + 0.0468 C_L^2$ |
| • Takeoff, gear up   | $C_D = 0.0264 + 0.0468 C_L^2$ |
| • Clean              | $C_D = 0.0124 + 0.0441 C_L^2$ |
| • Landing, gear up   | $C_D = 0.0764 + 0.0499 C_L^2$ |
| • Landing, gear down | $C_D = 0.0964 + 0.0499 C_L^2$ |



Table 3.6 Summary of the Geometry, Weight, Drag Polar, and  
Performance Sizing Data for the Mega-Transport  
(con't) (Ref. 40)

PERFORMANCE SIZING

• $C_{L_{max_{clean}}}$ , maximum clean lift coefficient.....	1.5
• $C_{L_{max_{TO}}}$ , maximum takeoff lift coefficient.....	2.3
• $C_{L_{max_L}}$ , maximum landing lift coefficient.....	2.8
• $T_{TO}$ , takeoff thrust required.....	400,000 lb
• $(T/W)_{TO}$ , takeoff thrust-to-weight ratio.....	0.28
• $(W/S)_{TO}$ , takeoff wing loading.....	120 lb/ft <sup>2</sup>

Table 3.7 Nondimensional Stability and Control Derivatives  
for the Mega-Transport (Ref. 40)

<u>FLIGHT CONDITION</u>	<u>Approach</u>	<u>Cruise</u>
Altitude (ft)	Sea Level	35,000
Air Density (slugs/ft <sup>3</sup> )	0.002377	0.0007365
Speed (Mach Number)	0.236	0.85
Initial Attitude (deg)	8.5	2.4
<u>WEIGHT AND INERTIAS</u>	<u>Approach</u>	<u>Cruise</u>
Weight (lb)	943,486	1,208,450
I <sub>xxB</sub> (slug-ft <sup>2</sup> )	73,588,769	94,255,050
I <sub>yyB</sub> (slug-ft <sup>2</sup> )	73,571,761	94,233,265
I <sub>zzB</sub> (slug-ft <sup>2</sup> )	147,477,302	188,894,047
I <sub>xzB</sub> (slug-ft <sup>2</sup> )	341,304	341,304
<u>STEADY STATE COEFFICIENTS</u>	<u>Approach</u>	<u>Cruise</u>
C <sub>L1</sub>	1.0194	0.4276
C <sub>D1</sub>	0.1627	0.0573
C <sub>TX1</sub>	0.1627	0.0573
C <sub>m1</sub>	0.0000	0.0000
C <sub>mT1</sub>	0.0000	0.0000

Table 3.7 Nondimensional Stability and Control Derivatives  
for the Mega-Transport (con't) (Ref. 40)

<u>LONGITUDINAL</u> <u>DERIVATIVES</u>	<u>Approach</u>	<u>Cruise</u>
$C_{m_u}$	0.0340	0.0806
$C_{m_\alpha}$	-1.1745	-1.1547
$C_{m_{\dot{\alpha}}}$	-5.2287	-8.7407
$C_{m_q}$	-18.5092	-22.8878
$C_{m_{T_u}}$	0.0000	0.0000
$C_{m_{T_\alpha}}$	0.0000	0.0000
$C_{L_u}$	0.0444	0.5038
$C_{L_\alpha}$	4.8560	6.3939
$C_{L_{\dot{\alpha}}}$	1.7338	2.8821
$C_{L_q}$	6.7542	8.4557
$C_{D_\alpha}$	0.4197	0.2318
$C_{D_u}$	0.0998	0.3592
$C_{T_{X_u}}$	0.0000	0.0000
$C_{L_{\delta_e}}$	0.4679	0.3088
$C_{D_{\delta_e}}$	0.0000	0.0000
$C_{m_{\delta_e}}$	-1.4111	-0.9365

Table 3.7 Nondimensional Stability and Control Derivatives  
for the Mega-Transport (con't) (Ref. 40)

<u>LATERAL-DIRECTIONAL</u> <u>DERIVATIVES</u>	<u>Approach</u>	<u>Cruise</u>
$C_{l\beta}$	-0.1887	-0.1944
$C_{lp}$	-0.6233	-0.5713
$C_{lr}$	0.3473	0.2388
$C_{l\delta_a}$	0.0525	0.0871
$C_{l\delta_r}$	0.0087	0.0157
$C_{n\beta}$	0.0758	0.1022
$C_{np}$	-0.1784	-0.0666
$C_{nr}$	-0.1604	-0.1756
$C_{n\delta_a}$	-0.0068	-0.0048
$C_{n\delta_r}$	-0.1149	-0.0714
$C_{y\beta}$	-0.6307	-0.7177
$C_{yp}$	-0.0301	-0.1001
$C_{yr}$	0.3993	0.4564
$C_{y\delta_a}$	0.0000	0.0000
$C_{y\delta_r}$	0.3001	0.1903

### Table 3.8 Longitudinal Transfer Functions for the Mega-Transport - Cruise Condition

POLYNOMIAL ANGLE OF ATTACK TO ELEVATOR TRANSFER FUNCTION

$$- 24.4565 S^3 - 1009.6143 S^2 - 33.0965 S - 5.1088$$

---


$$+ 832.0963 S^4 + 1386.7136 S^3 + 1649.0460 S^2 + 57.5235 S + 8.2503$$

FACTORED ANGLE OF ATTACK TO ELEVATOR TRANSFER FUNCTION

$$-24.4565 (S + 41.2493)(S^2 + 0.0327 S + 0.0051)$$

---


$$832.0963 (S^2 + 1.6350 S + 1.9251)(S^2 + 0.0315 S + 0.0052)$$

ANGLE OF ATTACK TO ELEVATOR TRANSFER FUNCTION  $K_{\text{gain}} = -0.619225$

POLYNOMIAL SPEED TO ELEVATOR TRANSFER FUNCTION

$$- 379.2522 S^2 + 16501.2675 S + 18726.0251$$

---


$$+ 832.0963 S^4 + 1386.7136 S^3 + 1649.0460 S^2 + 57.5235 S + 8.2503$$

FACTORED SPEED TO ELEVATOR TRANSFER FUNCTION

$$-379.2522 (S - 44.6167)(S + 1.1067)$$

---


$$832.0963 (S^2 + 1.6350 S + 1.9251)(S^2 + 0.0315 S + 0.0052)$$

SPEED TO ELEVATOR TRANSFER FUNCTION  $K_{\text{gain}} = 2269.729099$

POLYNOMIAL PITCH ATTITUDE TO ELEVATOR TRANSFER FUNCTION

$$- 1010.9590 S^2 - 622.9487 S - 22.7658$$

---


$$+ 832.0963 S^4 + 1386.7136 S^3 + 1649.0460 S^2 + 57.5235 S + 8.2503$$

FACTORED PITCH ATTITUDE TO ELEVATOR TRANSFER FUNCTION

$$-1010.9590 (S + 0.5772)(S + 0.0390)$$

---


$$832.0963 (S^2 + 1.6350 S + 1.9251)(S^2 + 0.0315 S + 0.0052)$$

PITCH ATTITUDE TO ELEVATOR TRANSFER FUNCTION  $K_{\text{gain}} = -2.759377$

Table 3.9 Longitudinal Mode Flying Quality Parameters  
and Flying Quality Levels for the Mega-Transport -  
Cruise Condition

LONGITUDINAL MODE CHECKING PARAMETERS

SHORT PERIOD UNDAMPED NATURAL FREQUENCY  
 $w_{n\_SP} = 1.3875 \text{ rad/s}$   
 SHORT PERIOD MODE DAMPING RATIO  
 $z_{SP} = 0.5892$   
 PHUGOID MODE UNDAMPED NATURAL FREQUENCY  
 $w_{n\_P} = 0.0718 \text{ rad/s}$   
 PHUGOID MODE DAMPING RATIO  
 $z_P = 0.2197$   
 DIMENSIONAL VARIATION OF  $Z_s$ -FORCE WITH ANGLE OF ATTACK  
 $z_a = -510.9474 \text{ ft/s}^2$   
 CURRENT ALTITUDE  
 Altitude = 35000 ft  
 CLASSIFICATION OF AIRPLANE  
 Class = 3  
 STEADY STATE NORMAL ACCELERATION CHANGE PER UNIT ALPHA  
 $n/a = 16.055 \text{ g/rad}$   
 TIME TO HALVE THE AMPLITUDE IN PHUGOID MODE  
 $T_{1/2\_P} = 43.959 \text{ s}$

FLYING QUALITY LEVELS FOR PHUGOID AND SHORT PERIOD

FLIGHT PHASE	PHUGOID LEVEL	LEVEL $z_{SP}$	LEVEL $w_{n\_SP}$
A	STABLE	I	BELOW LEVEL III
B	STABLE	I	I
C	STABLE	I	II

Table 3.10 Longitudinal Transfer Functions for the  
Mega-Transport - Approach Condition

POLYNOMIAL ANGLE OF ATTACK TO ELEVATOR TRANSFER FUNCTION

$$\begin{aligned} & - 15.7158 S^3 - 202.1180 S^2 - 1.5296 S - 6.6139 \\ & \hline & + 267.8360 S^4 + 437.9218 S^3 + 301.2720 S^2 + 9.2127 S + 5.8599 \end{aligned}$$

FACTORED ANGLE OF ATTACK TO ELEVATOR TRANSFER FUNCTION

$$\begin{aligned} & -15.7158 (S + 12.8558)(S^2 + 0.0050 S + 0.0327) \\ & \hline & 267.8360 (S^2 + 1.6332 S + 1.1021)(S^2 + 0.0018 S + 0.0199) \end{aligned}$$

ANGLE OF ATTACK TO ELEVATOR TRANSFER FUNCTION  $K_{\text{gain}} = -1.128665$

POLYNOMIAL SPEED TO ELEVATOR TRANSFER FUNCTION

$$\begin{aligned} & - 316.5542 S^2 + 2463.7369 S + 3877.5622 \\ & \hline & + 267.8360 S^4 + 437.9218 S^3 + 301.2720 S^2 + 9.2127 S + 5.8599 \end{aligned}$$

FACTORED SPEED TO ELEVATOR TRANSFER FUNCTION

$$\begin{aligned} & -316.5542 (S - 9.1253)(S + 1.3423) \\ & \hline & 267.8360 (S^2 + 1.6332 S + 1.1021)(S^2 + 0.0018 S + 0.0199) \end{aligned}$$

SPEED TO ELEVATOR TRANSFER FUNCTION  $K_{\text{gain}} = 661.706434$

POLYNOMIAL PITCH ATTITUDE TO ELEVATOR TRANSFER FUNCTION

$$\begin{aligned} & - 203.1635 S^2 - 122.5579 S - 5.6791 \\ & \hline & + 267.8360 S^4 + 437.9218 S^3 + 301.2720 S^2 + 9.2127 S + 5.8599 \end{aligned}$$

FACTORED PITCH ATTITUDE TO ELEVATOR TRANSFER FUNCTION

$$\begin{aligned} & -203.1635 (S + 0.5527)(S + 0.0506) \\ & \hline & 267.8360 (S^2 + 1.6332 S + 1.1021)(S^2 + 0.0018 S + 0.0199) \end{aligned}$$

PITCH ATTITUDE TO ELEVATOR TRANSFER FUNCTION  $K_{\text{gain}} = -0.969132$

Table 3.11 Longitudinal Mode Flying Quality Parameters  
and Flying Quality Levels for the Mega-Transport -  
Approach Condition

LONGITUDINAL MODE CHECKING PARAMETERS

SHORT PERIOD UNDAMPED NATURAL FREQUENCY  
 $w_{n\_SP} = 1.0498 \text{ rad/s}$   
 SHORT PERIOD MODE DAMPING RATIO  
 $z_{SP} = 0.7779$   
 PHUGOID MODE UNDAMPED NATURAL FREQUENCY  
 $w_{n\_P} = 0.1409 \text{ rad/s}$   
 PHUGOID MODE DAMPING RATIO  
 $z_P = 0.0064$   
 DIMENSIONAL VARIATION OF  $z_s$ -FORCE WITH ANGLE OF ATTACK  
 $z_a = -168.5652 \text{ ft/s}^2$   
 CURRENT ALTITUDE  
 Altitude = 0 ft  
 CLASSIFICATION OF AIRPLANE  
 Class = 3  
 STEADY STATE NORMAL ACCELERATION CHANGE PER UNIT ALPHA  
 $n/a = 5.239 \text{ g/rad}$   
 TIME TO HALVE THE AMPLITUDE IN PHUGOID MODE  
 $T_{1/2\_P} = 774.602 \text{ s}$

FLYING QUALITY LEVELS FOR PHUGOID AND SHORT PERIOD

FLIGHT PHASE	PHUGOID LEVEL	LEVEL $z_{SP}$	LEVEL $w_{n\_SP}$
A	STABLE	I	II
B	STABLE	I	I
C	STABLE	I	I



Table 3.12 Lateral-Directional Transfer Functions for the  
Mega-Transport - Cruise Condition

POLYNOMIAL SIDESLIP TO AILERON TRANSFER FUNCTION

$$\frac{+ 40.7242 S^2 + 96.3316 S + 4.4211}{+ 824.8455 S^4 + 1122.6774 S^3 + 725.6468 S^2 + 649.9309 S + 3.0385}$$

FACTORED SIDESLIP TO AILERON TRANSFER FUNCTION

$$\frac{40.7242 (S + 2.3186)(S + 0.0468)}{824.8455 (S + 1.1794)(S + 0.0047)(S^2 + 0.1770 S + 0.6646)}$$

SIDESLIP TO AILERON TRANSFER FUNCTION K\_gain = 1.455014

POLYNOMIAL SIDESLIP TO RUDDER TRANSFER FUNCTION

$$\frac{+ 15.0416 S^3 + 319.1989 S^2 + 345.7684 S - 4.4635}{+ 824.8455 S^4 + 1122.6774 S^3 + 725.6468 S^2 + 649.9309 S + 3.0385}$$

FACTORED SIDESLIP TO RUDDER TRANSFER FUNCTION

$$\frac{15.0416 (S - 0.0128)(S + 20.0752)(S + 1.1586)}{824.8455 (S + 1.1794)(S + 0.0047)(S^2 + 0.1770 S + 0.6646)}$$

SIDESLIP TO RUDDER TRANSFER FUNCTION K\_gain = -1.468971

POLYNOMIAL ROLL TO AILERON TRANSFER FUNCTION

$$\frac{+ 727.0867 S^2 + 164.9225 S + 341.6209}{+ 824.8455 S^4 + 1122.6774 S^3 + 725.6468 S^2 + 649.9309 S + 3.0385}$$

FACTORED ROLL TO AILERON TRANSFER FUNCTION

$$\frac{727.0867 (S^2 + 0.2268 S + 0.4698)}{824.8455 (S + 1.1794)(S + 0.0047)(S^2 + 0.1770 S + 0.6646)}$$

ROLL TO AILERON TRANSFER FUNCTION K\_gain = 112.429794

Table 3.12 Lateral-Directional Transfer Functions for the  
Mega-Transport - Cruise Condition (con't)

POLYNOMIAL ROLL TO RUDDER TRANSFER FUNCTION

$$\begin{aligned} &+ 148.9480 S^2 - 135.7998 S - 522.8862 \\ &----- \\ &+ 824.8455 S^4 + 1122.6774 S^3 + 725.6468 S^2 + 649.9309 S + 3.0385 \end{aligned}$$

FACTORED ROLL TO RUDDER TRANSFER FUNCTION

$$\begin{aligned} &148.9480 (S - 2.3842)(S + 1.4724) \\ &----- \\ &824.8455 (S + 1.1794)(S + 0.0047)(S^2 + 0.1770 S + 0.6646) \end{aligned}$$

ROLL TO RUDDER TRANSFER FUNCTION  $K_{\text{gain}} = -172.085442$

POLYNOMIAL HEADING TO AILERON TRANSFER FUNCTION

$$\begin{aligned} &- 42.4236 S^3 - 72.0698 S^2 - 5.3778 S + 12.9484 \\ &----- \\ &+ 824.8455 S^4 + 1122.6774 S^3 + 725.6468 S^2 + 649.9309 S + 3.0385 \end{aligned}$$

FACTORED HEADING TO AILERON TRANSFER FUNCTION

$$\begin{aligned} &-42.4236 (S - 0.3558)(S + 1.4718)(S + 0.5828) \\ &----- \\ &824.8455 (S + 1.1794)(S + 0.0047)(S^2 + 0.1770 S + 0.6646) \end{aligned}$$

HEADING TO AILERON TRANSFER FUNCTION  $K_{\text{gain}} = 4.261410$

POLYNOMIAL HEADING TO RUDDER TRANSFER FUNCTION

$$\begin{aligned} &- 302.5823 S^3 - 351.4678 S^2 - 11.8264 S - 19.9228 \\ &----- \\ &+ 824.8455 S^4 + 1122.6774 S^3 + 725.6468 S^2 + 649.9309 S + 3.0385 \end{aligned}$$

FACTORED HEADING TO RUDDER TRANSFER FUNCTION

$$\begin{aligned} &-302.5823 (S + 1.1759)(S^2 + -0.0144 S + 0.0560) \\ &----- \\ &824.8455 (S + 1.1794)(S + 0.0047)(S^2 + 0.1770 S + 0.6646) \end{aligned}$$

HEADING TO RUDDER TRANSFER FUNCTION  $K_{\text{gain}} = -6.556724$

Table 3.13 Lateral-Directional Roll Performance Parameters  
and Flying Quality Levels for the Mega-Transport -  
Cruise Condition

**ROLL PERFORMANCE CHECKING PARAMETERS**

CURRENT ALTITUDE  
 Altitude = 35000 ft  
 STEADY STATE FLIGHT SPEED  
 U<sub>1</sub> = 489.65 kts  
 WING AREA  
 S<sub>w</sub> = 11900.00 ft<sup>2</sup>  
 WING SPAN  
 b<sub>w</sub> = 318.04 ft  
 AIRPLANE MOMENT OF INERTIA ABOUT THE X-STABILITY AXIS  
 I<sub>xx\_s</sub> = 94616452 slgft<sup>2</sup>  
 ROLLING-MOMENT-DUE-TO-ROLL-RATE DERIVATIVE  
 C<sub>l\_p</sub> = -0.5713 1/rad  
 ROLLING-MOMENT-DUE-TO-AILERON DERIVATIVE  
 C<sub>l\_d\_a</sub> = 0.0871 1/rad  
 ROLL MODE TIME CONSTANT  
 TC<sub>ROLL</sub> = 0.848 s  
 AILERON DEFLECTION ANGLE  
 del<sub>a</sub> = 25.000 deg

**FLYING QUALITY LEVELS FOR THE ROLL MODE**

FLIGHT PHASE	ROLL TIME LEVEL	ROLL PERF. LEVEL
A	I	II
B	I	II
C	I	I

Table 3.14 Lateral-Directional Spiral and Dutch Roll  
Parameters and Flying Quality Levels for the  
Mega-Transport - Cruise Condition

**SPIRAL AND DUTCH ROLL PERFORMANCE CHECKING PARAMETERS**

```

CURRENT ALTITUDE
Altitude = 35000 ft
STEADY STATE FLIGHT SPEED
U1 = 489.65 kts
WING AREA
Sw = 11900.00 ft^2
WING SPAN
bw = 318.04 ft
AIRPLANE MOMENT OF INERTIA ABOUT THE X-STABILITY AXIS
Ixx_S = 94616452 slgft2
AIRPLANE MOMENT OF INERTIA ABOUT THE Z-STABILITY AXIS
Izz_S = 188532645 slgft2
AIRPLANE PRODUCT OF INERTIA IN XZ-STABILITY AXES
Ixz_S = -5847104 slgft2
YAWING-MOMENT-DUE-TO-SIDESLIP DERIVATIVE
Cn_B = 0.1022 1/rad
YAWING-MOMENT-DUE-TO-ROLL-RATE DERIVATIVE
Cn_p = -0.0666 1/rad
YAWING-MOMENT-DUE-TO-YAW-RATE DERIVATIVE
Cn_r = -0.1756 1/rad
ROLLING-MOMENT-DUE-TO-SIDESLIP DERIVATIVE
Cl_B = -0.1944 1/rad
ROLLING-MOMENT-DUE-TO-ROLL-RATE DERIVATIVE
Cl_p = -0.5713 1/rad
ROLLING-MOMENT-DUE-TO-YAW-RATE DERIVATIVE
Cl_r = 0.2388 1/rad
DUTCH ROLL UNDAMPED NATURAL FREQUENCY
wn_D = 0.8152 rad/s
DUTCH ROLL MODE DAMPING RATIO
zD = 0.1086
SPIRAL MODE TIME CONSTANT
TC_SPIRAL = 212.783 s
CLASSIFICATION OF AIRPLANE
Class = 3
MAXIMUM BANK ANGLE TO MAXIMUM SIDESLIP RATIO DURING DUTCH ROLL
|Phi/B|D = 1.8844
TIME TO DOUBLE THE AMPLITUDE IN SPIRAL MODE
T2_S = 147.490 s

```

**FLYING QUALITY LEVELS FOR SPIRAL AND DUTCH ROLL MODE**

FLIGHT PHASE	SPIRAL LEVEL	LEVEL w <sub>n_D</sub>	LEVEL z <sub>D</sub>	LEVEL (z <sub>D</sub> *w <sub>n_D</sub> )
A	I	I	II	II
B	I	I	I	II
C	I	I	I	II

Table 3.15 Lateral-Directional Transfer Functions for the  
Mega-Transport - Approach Condition

POLYNOMIAL SIDESLIP TO AILERON TRANSFER FUNCTION

$$\frac{+ 9.1638 S^2 + 25.3714 S + 1.0306}{+ 258.1840 S^4 + 490.3246 S^3 + 235.6321 S^2 + 146.2961 S + 0.6694}$$

FACTORED SIDESLIP TO AILERON TRANSFER FUNCTION

$$\frac{9.1638 (S + 2.7274)(S + 0.0412)}{258.1840 (S + 1.5451)(S + 0.0046)(S^2 + 0.3494 S + 0.3640)}$$

SIDESLIP TO AILERON TRANSFER FUNCTION K\_gain = 1.539566

POLYNOMIAL SIDESLIP TO RUDDER TRANSFER FUNCTION

$$\frac{+ 9.8836 S^3 + 82.1551 S^2 + 107.1098 S - 6.5702}{+ 258.1840 S^4 + 490.3246 S^3 + 235.6321 S^2 + 146.2961 S + 0.6694}$$

FACTORED SIDESLIP TO RUDDER TRANSFER FUNCTION

$$\frac{9.8836 (S - 0.0587)(S + 6.6734)(S + 1.6975)}{258.1840 (S + 1.5451)(S + 0.0046)(S^2 + 0.3494 S + 0.3640)}$$

SIDESLIP TO RUDDER TRANSFER FUNCTION K\_gain = -9.814506

POLYNOMIAL ROLL TO AILERON TRANSFER FUNCTION

$$\frac{+ 56.9494 S^2 + 13.0235 S + 6.7117}{+ 258.1840 S^4 + 490.3246 S^3 + 235.6321 S^2 + 146.2961 S + 0.6694}$$

FACTORED ROLL TO AILERON TRANSFER FUNCTION

$$\frac{56.9494 (S^2 + 0.2287 S + 0.1179)}{258.1840 (S + 1.5451)(S + 0.0046)(S^2 + 0.3494 S + 0.3640)}$$

ROLL TO AILERON TRANSFER FUNCTION K\_gain = 10.025851

Table 3.15 Lateral-Directional Transfer Functions for the  
Mega-Transport - Approach Condition (con't)

POLYNOMIAL ROLL TO RUDDER TRANSFER FUNCTION

$$+ 21.7794 S^2 - 60.1188 S - 51.6889$$

---


$$+ 258.1840 S^4 + 490.3246 S^3 + 235.6321 S^2 + 146.2961 S + 0.6694$$

FACTORED ROLL TO RUDDER TRANSFER FUNCTION

$$21.7794 (S - 3.4485)(S + 0.6882)$$

---


$$258.1840 (S + 1.5451)(S + 0.0046)(S^2 + 0.3494 S + 0.3640)$$

ROLL TO RUDDER TRANSFER FUNCTION K\_gain = -77.212545

POLYNOMIAL HEADING TO AILERON TRANSFER FUNCTION

$$- 9.5908 S^3 - 19.7949 S^2 - 1.5449 S + 0.7599$$

---


$$+ 258.1840 S^4 + 490.3246 S^3 + 235.6321 S^2 + 146.2961 S + 0.6694$$

FACTORED HEADING TO AILERON TRANSFER FUNCTION

$$-9.5908 (S - 0.1561)(S + 1.9612)(S + 0.2588)$$

---


$$258.1840 (S + 1.5451)(S + 0.0046)(S^2 + 0.3494 S + 0.3640)$$

HEADING TO AILERON TRANSFER FUNCTION K\_gain = 1.135098

POLYNOMIAL HEADING TO RUDDER TRANSFER FUNCTION

$$- 66.2688 S^3 - 105.1347 S^2 - 3.7830 S - 5.9391$$

---


$$+ 258.1840 S^4 + 490.3246 S^3 + 235.6321 S^2 + 146.2961 S + 0.6694$$

FACTORED HEADING TO RUDDER TRANSFER FUNCTION

$$-66.2688 (S + 1.5861)(S^2 + 0.0004 S + 0.0565)$$

---


$$258.1840 (S + 1.5451)(S + 0.0046)(S^2 + 0.3494 S + 0.3640)$$

HEADING TO RUDDER TRANSFER FUNCTION K\_gain = -8.871804

Table 3.16 Lateral-Directional Roll Performance Parameters  
and Flying Quality Levels for the Mega-Transport -  
Approach Condition

ROLL PERFORMANCE CHECKING PARAMETERS

CURRENT ALTITUDE  
 Altitude = 0 ft  
 STEADY STATE FLIGHT SPEED  
 U<sub>1</sub> = 156.00 kts  
 WING AREA  
 S<sub>w</sub> = 11900.00 ft<sup>2</sup>  
 WING SPAN  
 b<sub>w</sub> = 318.04 ft  
 AIRPLANE MOMENT OF INERTIA ABOUT THE X-STABILITY AXIS  
 I<sub>xx\_s</sub> = 76622459 slgft<sup>2</sup>  
 ROLLING-MOMENT-DUE-TO-ROLL-RATE DERIVATIVE  
 C<sub>l\_p</sub> = -0.6233 1/rad  
 ROLLING-MOMENT-DUE-TO-AILERON DERIVATIVE  
 C<sub>l\_d\_a</sub> = 0.0525 1/rad  
 ROLL MODE TIME CONSTANT  
 TC<sub>ROLL</sub> = 0.647 s  
 AILERON DEFLECTION ANGLE  
 del<sub>a</sub> = 25.000 deg

FLYING QUALITY LEVELS FOR THE ROLL MODE

FLIGHT PHASE	ROLL TIME LEVEL	ROLL PERF. LEVEL
A	I	BELOW LEVEL III
B	I	BELOW LEVEL III
C	I	BELOW LEVEL III

Table 3.17 Lateral-Directional Spiral and Dutch Roll  
Parameters and Flying Quality Levels for the  
Mega-Transport - Approach Condition

**SPIRAL AND DUTCH ROLL PERFORMANCE CHECKING PARAMETERS**

```

CURRENT ALTITUDE
Altitude = 0 ft
STEADY STATE FLIGHT SPEED
U1 = 156.00 kts
WING AREA
Sw = 11900.00 ft2
WING SPAN
bw = 318.04 ft
AIRPLANE MOMENT OF INERTIA ABOUT THE X-STABILITY AXIS
Ixx_S = 76622459 slgft2
AIRPLANE MOMENT OF INERTIA ABOUT THE Z-STABILITY AXIS
Izz_S = 144443543 slgft2
AIRPLANE PRODUCT OF INERTIA IN XZ-STABILITY AXES
Ixz_S = -14662220 slgft2
YAWING-MOMENT-DUE-TO-SIDESLIP DERIVATIVE
Cn_B = 0.0758 1/rad
YAWING-MOMENT-DUE-TO-ROLL-RATE DERIVATIVE
Cn_p = -0.1784 1/rad
YAWING-MOMENT-DUE-TO-YAW-RATE DERIVATIVE
Cn_r = -0.1604 1/rad
ROLLING-MOMENT-DUE-TO-SIDESLIP DERIVATIVE
Cl_B = -0.1887 1/rad
ROLLING-MOMENT-DUE-TO-ROLL-RATE DERIVATIVE
Cl_p = -0.6233 1/rad
ROLLING-MOMENT-DUE-TO-YAW-RATE DERIVATIVE
Cl_r = 0.3473 1/rad
DUTCH ROLL UNDAMPED NATURAL FREQUENCY
wn_D = 0.6034 rad/s
DUTCH ROLL MODE DAMPING RATIO
zD = 0.2896
SPIRAL MODE TIME CONSTANT
TC SPIRAL = 216.929 s
CLASSIFICATION OF AIRPLANE
Class = 3
MAXIMUM BANK ANGLE TO MAXIMUM SIDESLIP RATIO DURING DUTCH ROLL
|Phi/B|D = 0.9439
TIME TO DOUBLE THE AMPLITUDE IN SPIRAL MODE
T2_S = 150.364 s

```

**FLYING QUALITY LEVELS FOR SPIRAL AND DUTCH ROLL MODE**

FLIGHT PHASE	SPIRAL LEVEL	LEVEL w <sub>n_D</sub>	LEVEL z <sub>D</sub>	LEVEL (z <sub>D</sub> *w <sub>n_D</sub> )
A	I	I	I	II
B	I	I	I	I
C	I	I	I	I



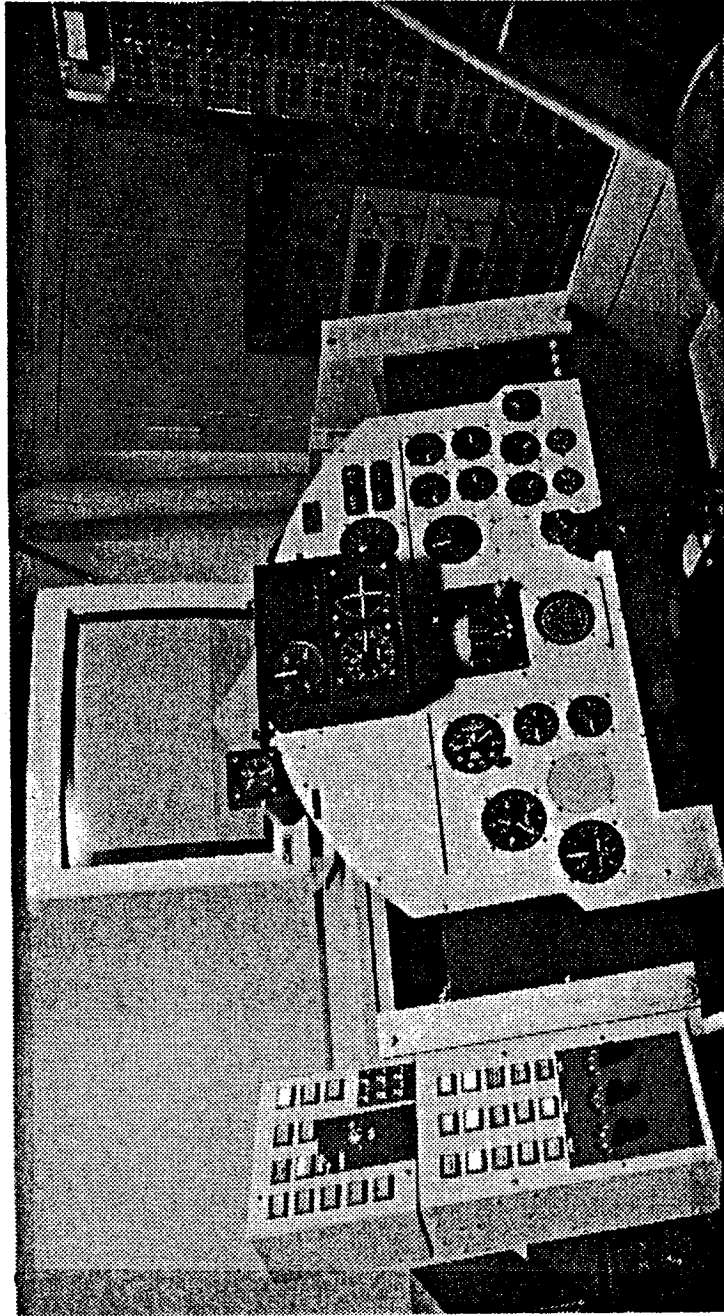
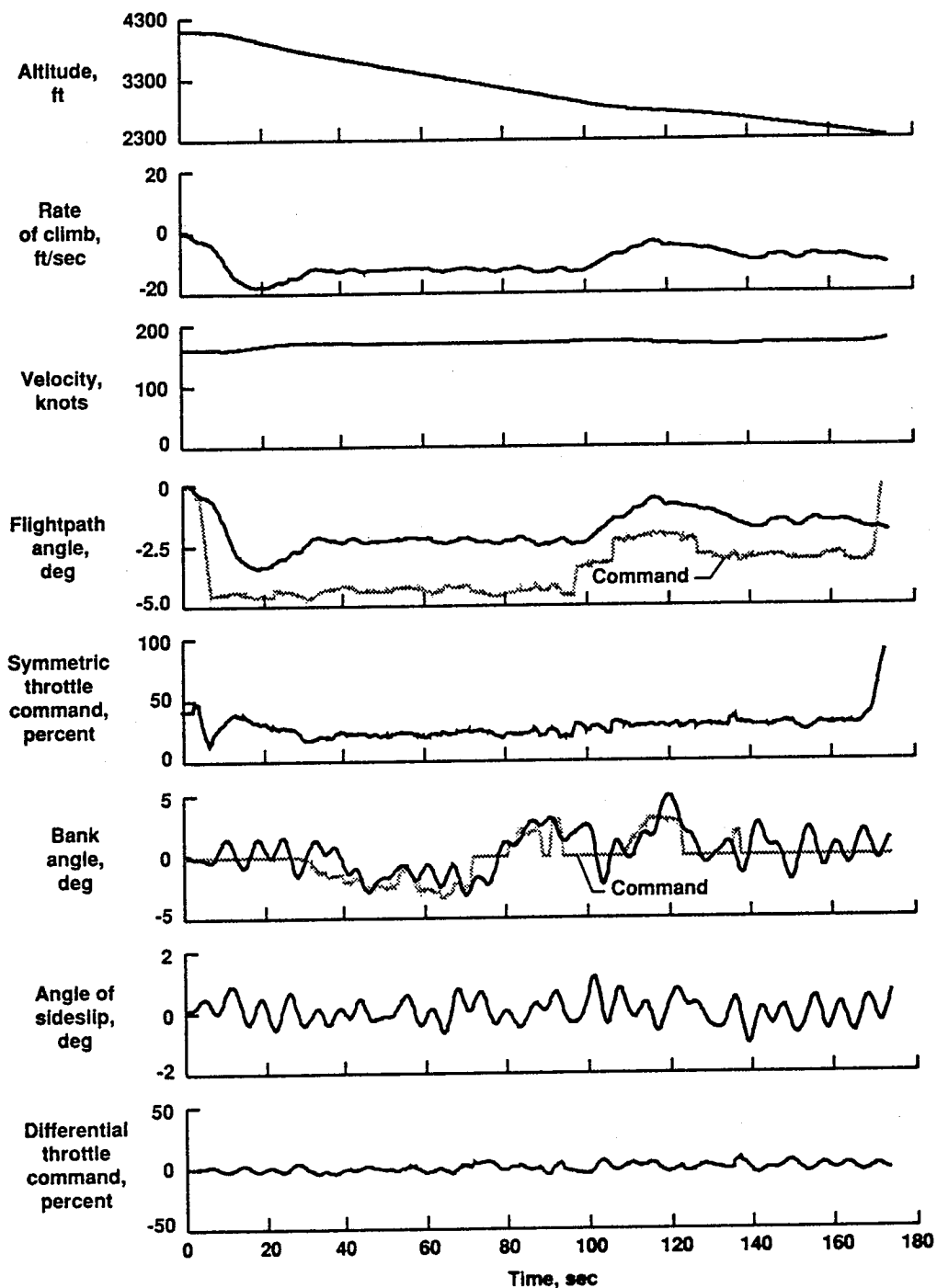


Figure 3.1 NASA Dryden B-720 Simulation Cockpit (Ref. 19)



**Figure 3.2 Time-History of B-720 Augmented Throttles-Only Control System Approach and Landing: 160 knots. No Flaps. Light Turbulence. 1,000 Foot Offset from Runway (Ref. 19)**

### MISSION PHASES

- 1) Warmup
- 2) Taxi
- 3) Takeoff to destination airport
- 4) Climb to cruise altitude
- 5) Cruise to destination airport
- 6) Loiter
- 7) Descent

- 8) Land/Taxi
- 9) Takeoff to alternate airport
- 10) Climb to intermediate altitude
- 11) Cruise to alternate airport
- 12) Loiter
- 13) Descent
- 14) Land/Taxi

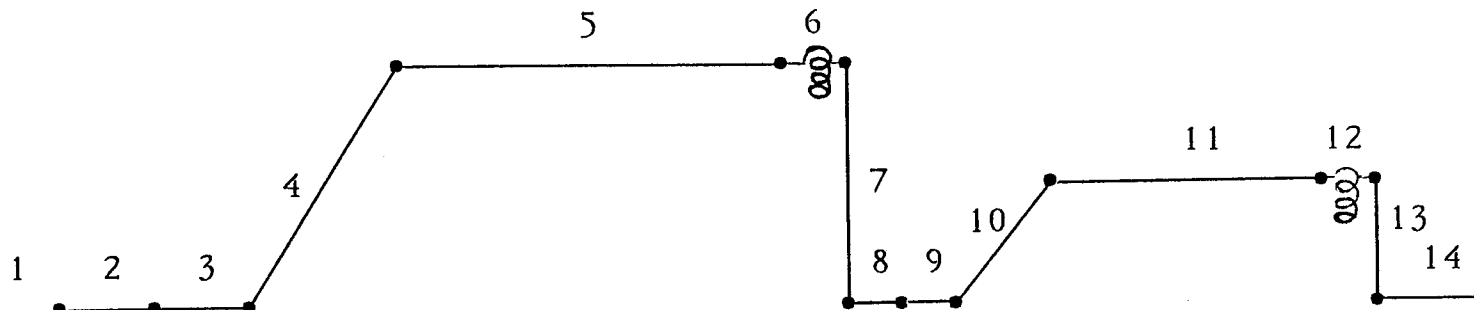


Figure 3.3 Mission Profile of the Mega-Transport (Ref. 40)

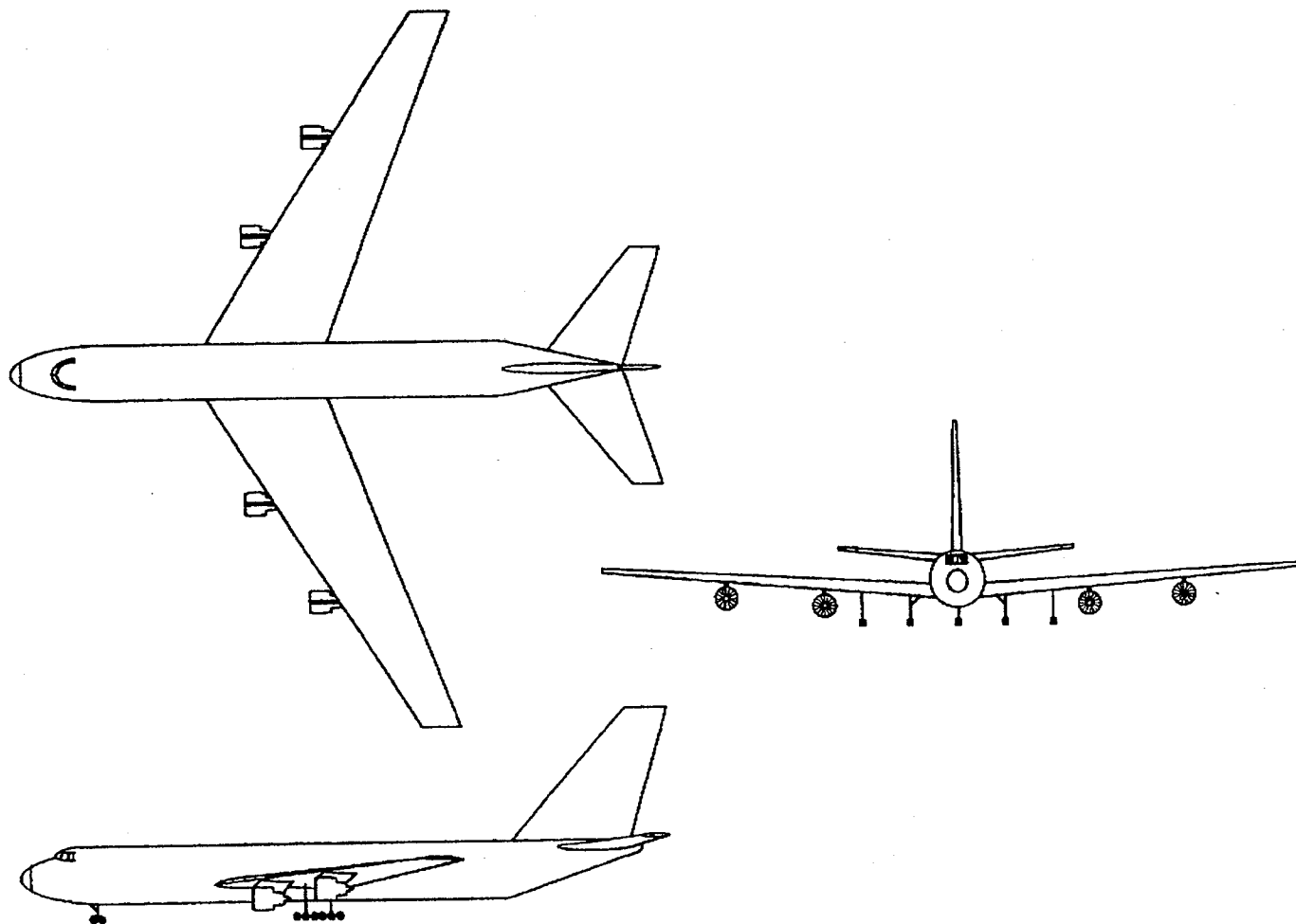
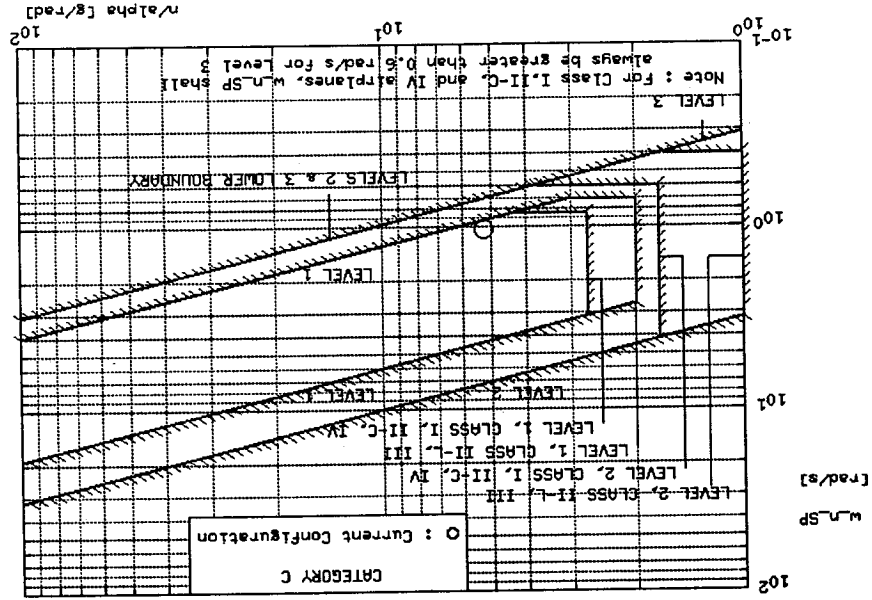


Figure 3.4 A Preliminary Three-View of the Mega-Transport

(Ref. 40)

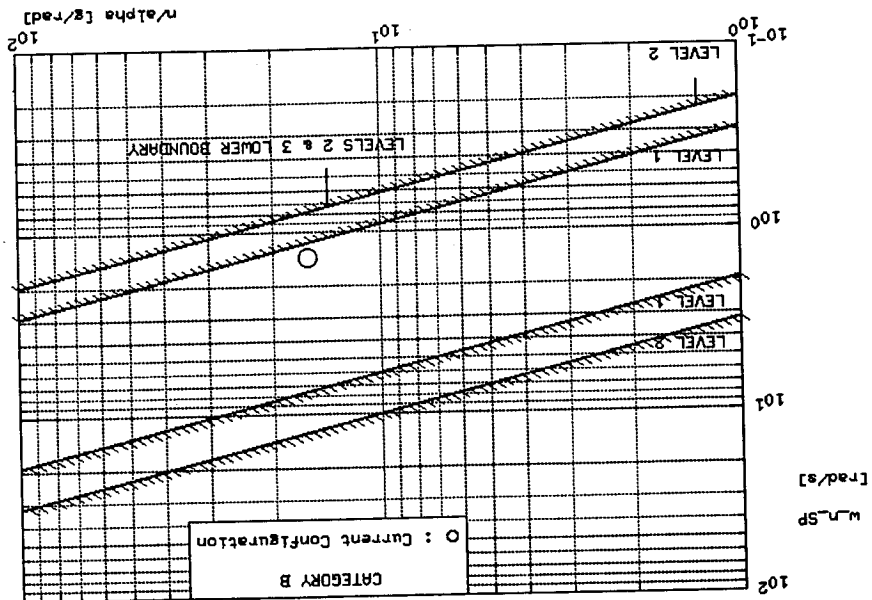
# Mega-Transport - Approach Condition

Figure 3.6 Short-Period Frequency Requirements for the



# Mega-Transport - Cruise Condition

Figure 3.5 Short-Period Frequency Requirements for the



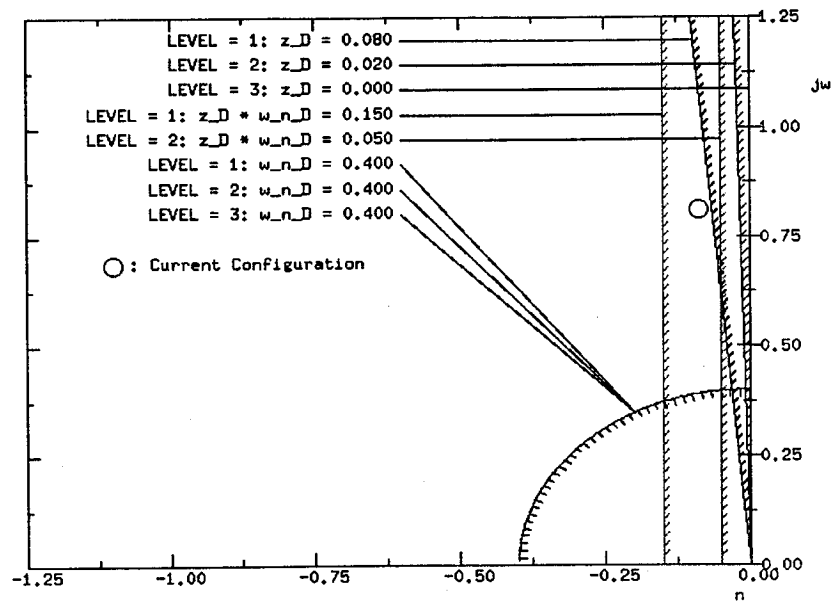


Figure 3.7 Minimum Dutch Roll Frequency and Damping Ratio Requirements for the Mega-Transport - Cruise Condition

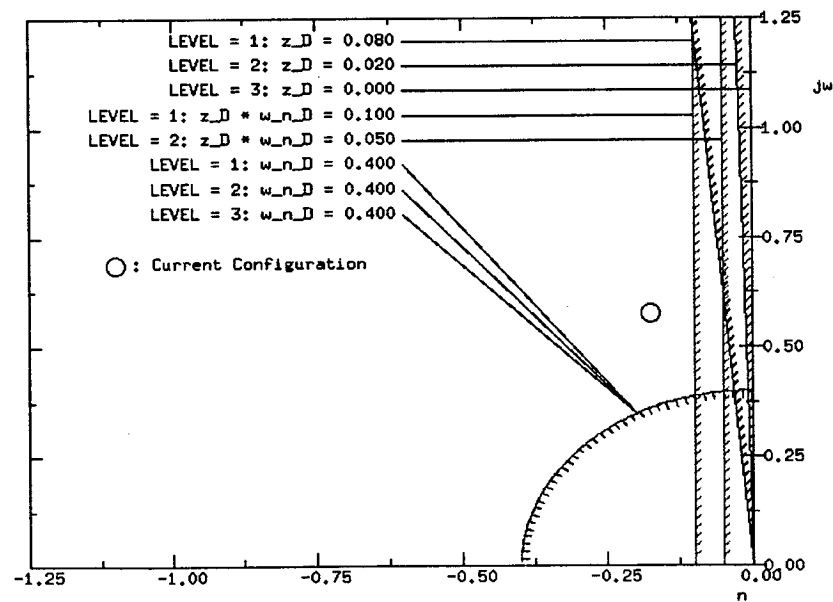


Figure 3.8 Minimum Dutch Roll Frequency and Damping Ratio Requirements for the Mega-Transport - Approach Condition

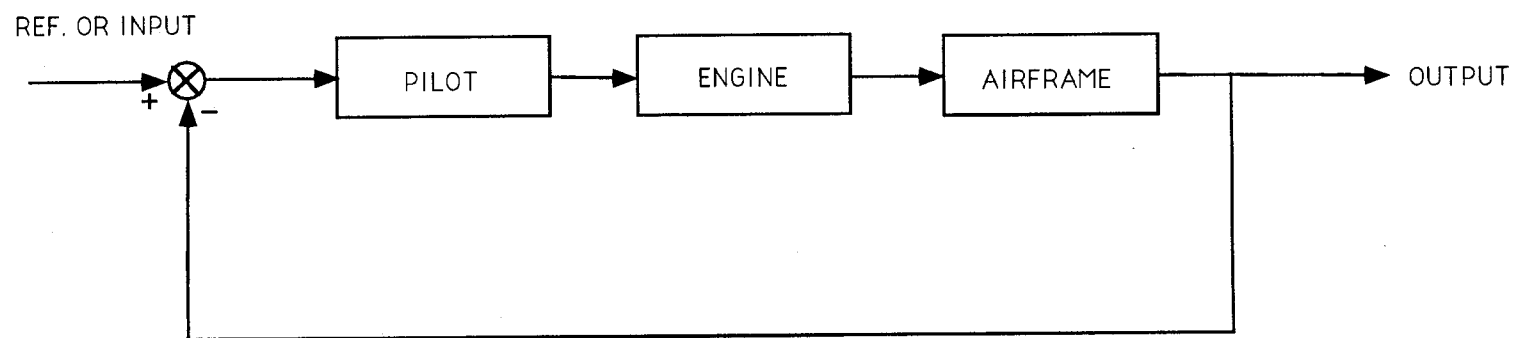


Figure 3.9 Pilot/Engine/Airframe Closed Loop System (Ref. 43)

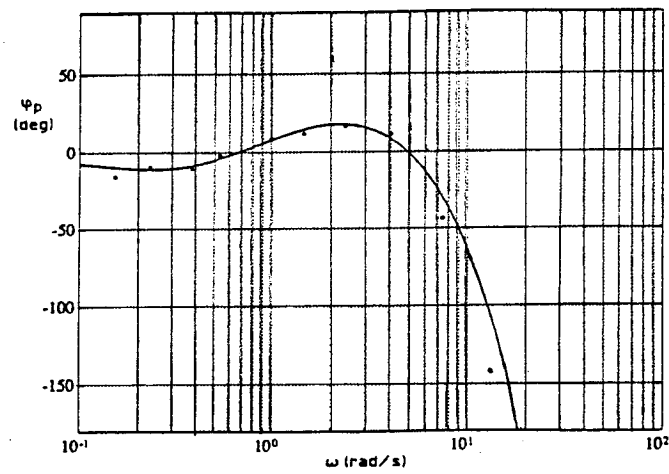
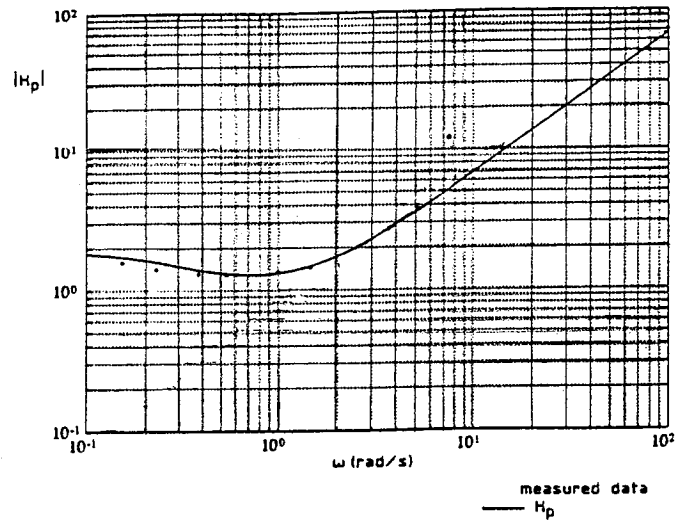


Figure 3.10 Measured Data with Fitted Pilot Model  $H_p(\omega)$  for  
Disturbance Task (Ref. 49)



## CHAPTER 4

### REFERENCES

1. National Transportation Safety Board, Aircraft Accident Report, PB90-910406, NTSB/AAR-90/06, United Airlines Flight 232, McDonnell-Douglas DC-10-10, Sioux Gateway Airport, Sioux City, Iowa, July 19, 1989.
2. Hughes, David, and Michael A. Dornheim, *United DC-10 Crashes in Sioux City, Iowa*, Aviation Week & Space Technology : Vol. 131, No. 4, 96 - 97, July 24, 1989.
3. Ott, James, *Probe Focuses on Failure of Fan Disk in DC-10 Crash*, Aviation Week & Space Technology : Vol. 131, No. 5, 30 - 31, July 31, 1989.
4. Ott, James, *Investigators Find Reconstructed Tail of DC-10 Riddled with Damage*, Aviation Week & Space Technology : Vol. 131, No. 6, 22 - 23, August 7, 1989.
5. Taylor, J.W.R. , Jane's All the World's Aircraft, Jane's Information Group, Sentinel House, 163 Brighton Rd., Coulsdon, Surrey, CR5 2NH, UK, 1984 - 1985.
6. Lacagnina, Mark, *Locked Controls at 37,000 Feet in a DC-10*, Aviation Safety : Vol. XI, No. 7, 4 - 6, April 1, 1991.

7. Burcham, F., Jr., C. Fullerton, G. Gilyard, T. Wolf, and J. Stewart, "A Preliminary Investigation of the Use of Throttles for Emergency Flight Control", NASA TM-4320, 1991.
8. Dornheim, Michael A., *NASA Develops Software to Control Aircraft With Throttles Alone*, Aviation Week & Space Technology : Vol. 134, No. 25, 42, June 24, 1991.
9. Gilyard, Glenn B., Joseph L. Conley, Jeanette L. Le, and Frank W. Burcham, Jr., "A Simulation Evaluation of a Four-Engine Jet Transport Using Engine Thrust Modulation for Flightpath Control", NASA TM-4324, September 1991.
10. Lenorovitz, Jeffrey M., *Airbus Survey Confirms Requirement For Very Large Transport Aircraft*, Aviation Week & Space Technology : Vol. 135, No. 18, 34 - 35, October 28, 1991.
11. *Boeing Seeking Carrier Input In Planning New Large Aircraft*, Aviation Week & Space Technology : Vol. 136, No. 1, 20 - 22, January 6, 1992.
12. *Various Cross Sections Evaluated for Large Transport*, Aviation Week & Space Technology : Vol. 136, No. 8, 35, February 24, 1992.
13. *Mass-Transporter*, Flight International : Vol. 141, No. 4312, 22 - 28, 1 - 7 April, 1992.

14. Smith, Bruce A., *Douglas Plans Shorter, Double-Deck MD-12*, Aviation Week & Space Technology : Vol. 136, No. 15, 18 - 19, April 13, 1992.
15. Smith, Bruce A., *Large Transport Could Mark New Era for Douglas Aircraft*, Aviation Week & Space Technology : Vol. 136, No. 18, 22 - 24, May 4, 1992.
16. Sparaco, Pierre, *Airbus Pursues 600-Seat UHCA Program*, Aviation Week & Space Technology : Vol. 137, No. 11, 39 - 41, September 14, 1992.
17. Roskam, Jan, Proposal to NASA Ames Research Center, Moffett Field, California, for Design, Analysis and Control of Large Transports so that Control of Engine Thrust Can be Used as a Back-up of the Primary Flight Controls, University of Kansas, Department of Aerospace Engineering, April 1992.
18. Burcham, Frank W. Jr. and C. Gordon Fullerton, "Controlling Crippled Aircraft - With Throttles", NASA TM-104238, 1991.
19. Burcham, Frank W., Jr., Trindel Maine, and Thomas Wolf, "Flight Testing and Simulation of an F-15 Airplane Using Throttles for Flight Control", NASA TM-104255, August 1992.
20. *NTSB Probes DC-10 Cargo Door Devices*, Aviation Week & Space Technology : Vol. 96, No. 25, 23, June 19, 1972.

21. *Cargo Door Focus of Paris Crash Study*, Aviation Week & Space Technology : Vol. 100, No. 10, 198 - 199, March 11, 1974.
22. *DC-10 Evidence Points to Cargo Door*, Aviation Week & Space Technology : Vol. 100, No. 13, 26 - 27, April 1, 1974.
23. *C-5 Crash Cause Sought*, Aviation Week & Space Technology : Vol. 102, No. 15, 18, April 14, 1975.
24. Internal memo at NASA Dryden Flight Research Facility, Edwards, California, from Bill Burcham concerning C-5 loss of flight control, May 29, 1992.
25. McMahan, Jack, *Flight 1080*, Air Line Pilot , July 1978.
26. *Japan Orders Checks of 747 Tail Sections After JAL Crash*, Aviation Week and Space Technology : Vol. 123, No. 7, 30, August 19, 1985.
27. *JAL Crash Inquiry Team Examining Damage in Aft Pressure Bulkhead*, Aviation Week and Space Technology : Vol. 123, No. 8, 28 - 30, August 26, 1985.
28. *JAL Crash Investigators Set to Transfer Wreckage*, Aviation Week and Space Technology : Vol. 123, No. 9, 33, September 2, 1985.

29. *Inquiry Committee Analyzes JAL 747 Flight Data Recorder*,  
Aviation Week and Space Technology : Vol. 123, No. 10, 97,  
September 9, 1985.
30. *747 Inquiry Team Examines Repaired Bulkhead Replicas*,  
Aviation Week and Space Technology : Vol. 123, No. 11, 31,  
September 16, 1985.
31. *Limited Repairs to Follow 747 Bulkhead Review*, Aviation Week  
and Space Technology : Vol. 123, No. 12, 28, September 23, 1985.
32. Roskam, Jan, Airplane Flight Dynamics and Automatic Flight  
Controls : Part I. Roskam Aviation and Engineering Corporation,  
120 East Ninth, Suite 2, Lawrence, Kansas, Second Printing, 1982.
33. NASA Dryden Flight Research Facility F-15 Simulation Data
34. Taylor, J.W.R. , Jane's All the World's Aircraft, Jane's Information  
Group, Sentinel House, 163 Brighton Rd., Coulsdon, Surrey, CR5  
2NH, UK, 1991 - 1992.
35. Propulsion Controlled Aircraft (PCA) MD-11 Simulator  
Demonstration briefing at Douglas Aircraft Company, Long Beach,  
California, August 6, 1992.
36. Internal memo at NASA Dryden Flight Research Facility,  
Edwards, California, from Bill Burcham concerning MD-11, Ship

506, Flight 51, September 13, 1992.

37. MIL-F-8785C (USAF), Military Specification - Flying Qualities of Piloted Airplanes, November 5, 1980.
38. Horton, Timothy W. and Robert W. Kempel, "Flight Test Experience and Controlled Impact of a Remotely Piloted Jet Transport Aircraft", NASA TM-4084, November 1988.
39. Advanced Aircraft Analysis Computer Program, Version 1.4, Design, Analysis and Research Corporation, 120 East Ninth St., Suite 2, Lawrence, Kansas, 66044, 1993.
40. Gerren, Donna S., Mission Weight Sizing, Takeoff Weight Sensitivities, and Performance Constraint Analysis for the Mega-Transport, University of Kansas/Dryden Flight Research Facility, September 1992.
41. FAR 121, Certification and Operations : Domestic, Flag, and Supplemental Air Carriers and Commercial Operators of Large Aircraft, Federal Aviation Agency, Washington, D.C., May 1981.
42. Walsh, K., "Summary of the Effects of Engine Throttle Response on Airplane Formation-Flying Qualities", AIAA-92-3318, July 1992.

43. Roskam, Jan, Airplane Flight Dynamics and Automatic Flight Controls : Part II. Roskam Aviation and Engineering Corporation, 120 East Ninth, Suite 2, Lawrence, Kansas, First Printing, 1979.
44. Bauerfeind, Klaus, "Some General Topics in the Field of Engine Handling", AGARD Conference Proceedings No. 324 - Engine Handling, Paper No. 1, October 11 - 14, 1982.
45. Koff, Bernard L., "Designing For Fighter Engine Transients", AGARD Conference Proceedings No. 324 - Engine Handling, Paper No. 2, October 11 - 14, 1982.
46. Patterson, Grant T., "Techniques For Determining Engine Stall Recovery Characteristics", AGARD Conference Proceedings No. 324 - Engine Handling, Paper No. 28, October 11 - 14, 1982.
47. McRuer, Duane, Dunstan Graham, Ezra Krendel, and William Reisener, Jr., "Human Pilot Dynamics in Compensatory Systems - Theory, Models, and Experiments with Controlled Element and Forcing Function Variations", AFFDL-TR-65-15, July 1965.
48. Torenbeek, E., "Development and Application of a Comprehensive, Design-Sensitive Weight Prediction Method for Wing Structures of Transport Category Aircraft", Report LR-693, Delft University Press, Delft, The Netherlands, September 1992.

49. Van der Vaart, Johannes C., "Modelling of Perception and Action in Compensatory Manual Control Tasks", Delft University Press, Delft, The Netherlands, 1992.